The Dissertation Committee for Ashley Diane Solmonson Certifies that this is the approved version of the following dissertation:

Molecular mechanisms opposing obesity and skin cancer in response to UCP3 overexpression in epidermis

Committee:

Edward M Mills, Supervisor

Dean Appling

John DiGiovanni

Karen M. Vasquez

Stefano Tiziani

Molecular mechanisms opposing obesity and skin cancer in response to UCP3 overexpression in epidermis

by

Ashley Diane Solmonson, B.S.

Dissertation

Presented to the Faculty of the Graduate School of

The University of Texas at Austin

in Partial Fulfillment

of the Requirements

for the Degree of

Doctor of Philosophy

The University of Texas at Austin

August 2016

Acknowledgements

I would like to thank my mentor Dr. Ted Mills for allowing me to join his lab and for giving me the opportunity to gain valuable experience and the resources to be successful early in my career. I would also like to thank members of my dissertation committee. I could not have asked for a better source of support than Drs. Dean Appling, John DiGiovanni, Karen Vasquez and Stefano Tiziani. You all were incredibly encouraging and provided wonderful guidance. I am thankful for the opportunity to have collaborated and learned from each of you.

I owe many thanks to Dr. Joyce Rundhaug, whom I could not have done much of this without. I'm so grateful for all the help you provided and the general kindness of your heart. I also want to thank Dr. Sara Nowinski for being a mentor and friend. I could not have asked for a better scientist to share a project with. We may have disagreed a once or twice but I truly appreciate the time that we were able to work together. I hope we can collaborate in the future!

To the many other Mills lab members I have had the privilege to work with over the years, I have many thanks. Chris Riley and Dr. Shohei Kohno, you both have created such a vibrant and fast paced environment that it is hard to keep up with you! You have both been wonderful resources for me and some of my very best drinking buddies and for that I thank you!

To Tiffany and the rest of the Grizwald clan, you all are the most wonderful people and you bring such joy and laughter into my life. Your support and love has been such a solid foundation for me to chase my dreams and for that I am forever grateful.

Molecular mechanisms opposing obesity and skin cancer in response to UCP3 overexpression in epidermis

Ashley Diane Solmonson, Ph.D.

The University of Texas at Austin, 2016

Supervisor: Edward M. Mills

The ability to increase energy expenditure by burning fats for heat production is a specialized characteristic of mammals that allows for maintenance of core body temperature in cold environments. The molecular mechanisms involved in thermogenesis include the actions of uncoupling proteins which facilitate inefficient conversion of nutrients into cellular energy allowing energy dissipation in the form of heat. Increased energy expenditure resulting from increased uncoupling protein 3 (UCP3) expression in skeletal muscle and adipose tissue can prevent obesity and lower body weight. Here, we demonstrate that UCP3 overexpression in basal epidermis is sufficient to prevent obesity and lower body weight. Furthermore, overexpression of UCP3 in epidermis increases overall glucose tolerance and insulin sensitivity through activation of the energy sensitive kinase, AMP-activated kinase (AMPK) and increased expression of the glucose transporter, Glut1. This provides a proof-of-principle that uncoupled respiration in skin may be a useful target in treating obesity and hyperglycemia.

UCP3 overexpression increases lipid oxidation in epidermis that opposes accumulation of biomass needed for keratinocyte proliferation. Studies within provide a link between increased lipid catabolism and inhibition of Akt as a new mechanism of metabolic regulation of cell signaling. UCP3-mediated lipid oxidation leads to altered membrane dynamics and reduced membrane localization of Akt. Inhibition of lipid oxidation rescues Akt activation when UCP3 is overexpressed and activates Akt in normal murine and human keratinocytes. Overexpression of Akt rescues proliferation and carcinogenesis in the presence of UCP3 overexpression in bitransgenic mice. These findings demonstrate that UCP3 overexpression can limit cell proliferation and tumorigenesis in epidermis by a mechanism where mitochondrial metabolism regulates growth signaling.

Table of Contents

List of Tables

List of Figures

List of Illustrations

Chapter 1: Introduction

1.1 Mechanisms of body weight regulation

Overall body weight is controlled by the balance of energy intake and energy expenditure. Energy intake in excess of energy expenditure leads to weight gain and long term leads to obesity. With obesity rates rising at an alarming rate, the need for novel therapeutic alternatives to reverse obesity and prevent consequential disease progression has never been greater. Over the past decade, genetic studies have greatly advanced our knowledge of mechanisms that regulate body weight. This has enhanced the development of therapeutics that target limiting energy intake or nutrient absorption, altering protein and fat storage, or increasing energy expenditure[1]. Fat storage evolved as a mechanism to protect body weight when energy intake is low, so many anti-obesity treatments reach a plateau of efficacy after an initial weight loss, as the body attempts to maintain metabolic homeostasis and fight further weight loss. This has increased interest in thermogenic mechanisms that increase fat oxidation and may be used in conjunction with current therapies. Here, I will present data suggesting that disruption of epidermal lipid metabolism can increase energy expenditure to reduce body weight and prevent obesity.

Total energy expenditure is comprised of the energy needed to maintain cellular adenosine triphosphate (ATP) levels or basal metabolic rate, and thermogenesis in which fat is burned for heat production. Basal metabolic rate can be increased with activity, and regular exercise has been promoted as a mechanism to increase basal metabolic rate and energy expenditure. However, the high caloric content of modern diets makes exercise

alone insufficient to combat obesity long term without dietary intervention. Interestingly, mechanisms that increase energy expenditure through thermogenesis have consistently demonstrated sufficiency to decrease body weight even with obesogenic diets[2,3]. A brief review of systemic metabolic regulation and cellular energy production follows to help explain our findings that increased energy expenditure in basal epidermis can lower body weight.

1.2 MECHANISMS OF ENERGY STORAGE

The rate of energy expenditure must be matched by homeostatic control of circulating nutrient availability and energy storage. In between feeding, animals maintain relatively tight circulating glucose levels even upon days of fasting that is achieved by release of energy stores from adipose tissue and hepatic glucose production. Energy storage and release is regulated through a complex network of metabolic hormones that modulate multiple organ systems simultaneously[4-6]. This subject has been reviewed elsewhere, so a brief discussion of the role of insulin in regulating fat storage and glucose homeostasis follows.

After a 24 hour fast, circulating insulin levels are low and blood glucose concentration is maintained by hepatic glucose production which matches glucose utilization by peripheral tissues. Adipose tissue undergoes lipolysis during fasting to release of free fatty acids that can be taken up by tissues that utilize β-oxidative pathways. After a meal, blood glucose levels rise and insulin is released, which promotes energy storage through both excitatory and inhibitory actions various tissues. In skeletal

muscle, insulin stimulates glucose uptake through glucose transporter 4 (GLUT4) to replenish local glycogen stores and stimulates protein synthesis. In adipose tissue, insulin stimulation also increases glucose uptake through GLUT4 to increase *de novo* lipogenesis and fat storage. Additionally, insulin inhibits adipose lipolysis, and promotes adipocyte proliferation to increase fat storage capacity. In liver, insulin stimulation inhibits gluconeogenesis and promotes glycogen and fatty acid synthesis. Liver converts excess glucose into triglycerides that can be transported to adipose tissue for long term storage.

These mechanisms of energy storage (summarized in Illustration 1) are dysregulated in Type 2 diabetes and result in hypoglycemia and hyperinsulinemia due to insulin resistance[7]. Increased thermogenesis has beneficial effects on whole body metabolism by improved glucose tolerance and insulin sensitivity reduced fat accumulation[2,8]. Thermogenic mechanisms that promote this effect function at the level of mitochondria reducing the efficiency of ATP production, driving increased nutrient demand by thermogenic tissues.

1.2 MECHANISMS OF ENERGY PRODUCTION

Generally, cells utilize glucose or free fatty acids derived from circulation to produce energy in the form of ATP in mitochondria. Many tissues contain cells that can switch from glucose oxidation to fatty acid oxidation when glucose levels are low (e.g. during fasting). These peripheral tissues can then switch back to utilizing glucose for energy

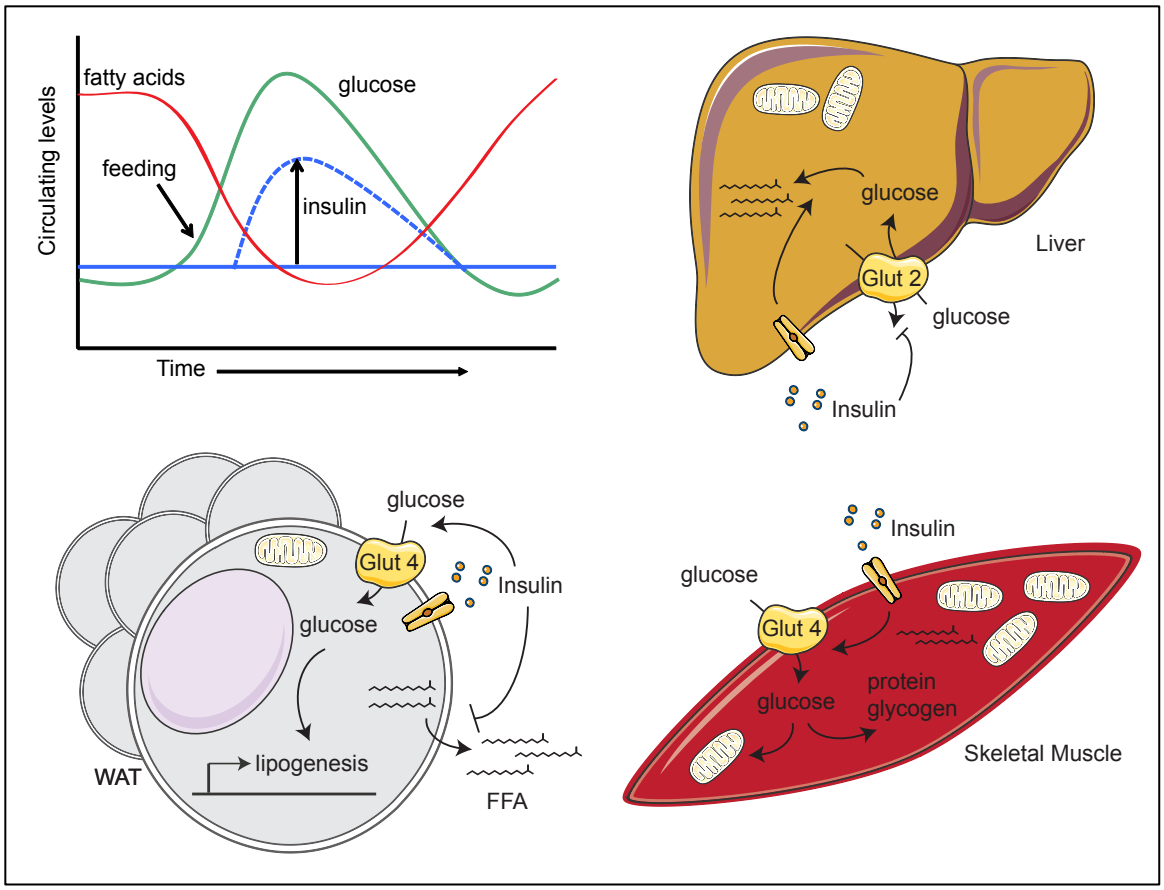

Illustration 1. Mechanisms of energy storage by insulin

Insulin negatively controls circulating glucose levels by inhibiting hepatic glucose production and promoting fatty acid synthesis in liver. In white adipose tissue, insulin inhibits lipolysis and free fatty acid (FFA) release and promotes energy storage by increasing lipogenesis and triglyceride synthesis. In skeletal muscle, insulin stimulation promotes glucose uptake and replenishment of local glycogen and protein stores.

production when circulating glucose is increased (e.g. feeding). Glucose enters cells through glucose transport proteins (GLUTs) at the cell membrane and is oxidized using the glycolytic pathway converting the 6 carbon sugar into (2) 3 carbon intermediates of pyruvate, generating a net 2 ATP in the process[9]. Pyruvate is a versatile intermediate that can be completely oxidized to carbon dioxide (CO_2) in mitochondria, converted to lactate and secreted from the cell, or utilized for biosynthetic reactions. Pyruvate destined for energy production enters the mitochondria through the mitochondrial pyruvate carrier (MPC) and is converted into acetyl CoA by the actions of pyruvate dehydrogenase (PDH)[10]. Mitochondrial acetyl CoA can also be produced through β-oxidation of fatty acids. Fatty acids stored as triglycerides in adipose tissue are released upon fasting or in times of high energy demand (e.g. cold exposure, exercise). Cells in peripheral tissues import fats from circulation using membrane transport proteins (CD36/FATp) and into mitochondria using the mitochondrial carnitine shuttle[6]. Carnitine palmitoyl-transferase 1 (CPT1) conjugates a fatty acyl-CoA to carnitine to produce an acyl-carnitine which can be transported into the mitochondrial matrix by a translocase where carnitine palmitoyl transferase 2 (CPT2) converts the acyl-carnitine back to a fatty acyl-CoA and free carnitine. The fatty acyl-CoA can then enter the β-oxidation pathway to generate acetyl CoA, and the free carnitine is transported out of the matrix for continued utilization by the shuttle system (Illustration 2)[11].

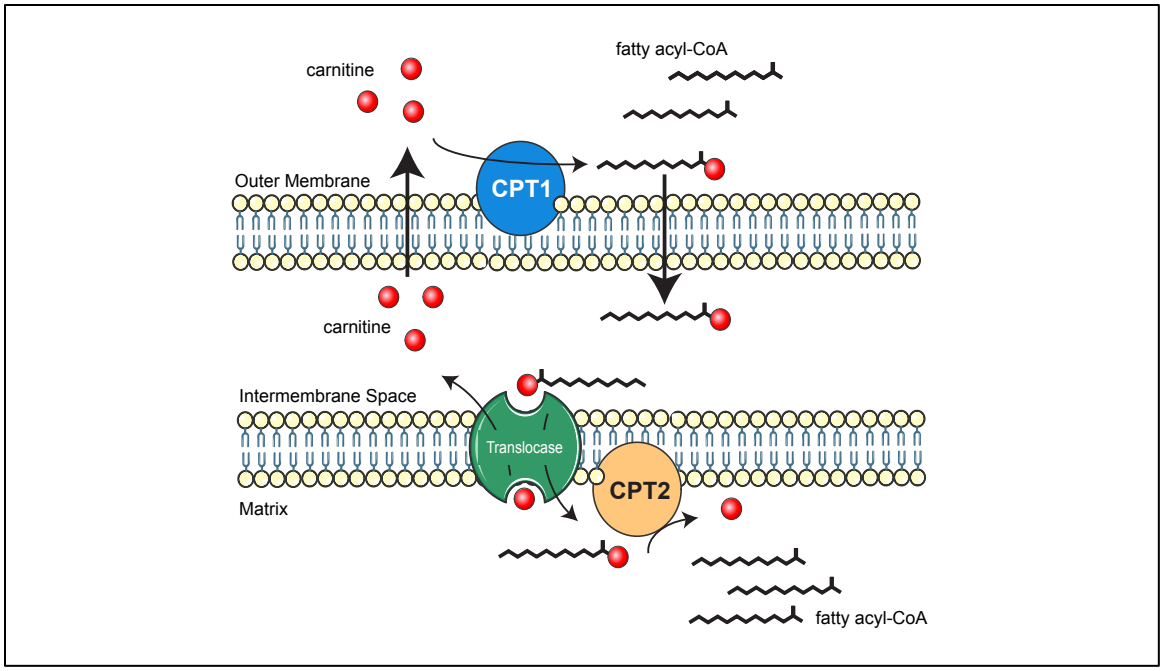

Illustration 2. The carnitine shuttle for mitochondrial fatty acid import

Fatty acyl CoA is conjugated to carnitine by carnitine palmitoyltransferase 1 (CPT1) on the outer mitochondrial membrane. The outer membrane is permeable to acyl-carnitines which are then transported into the mitochondrial matrix by a translocase where carnitine palmitoyltransferase 2 (CPT2) then removes the carnitine and releases a free fatty acyl CoA into the mitochondrial matrix where it can enter the β-oxidation pathway. The translocase transports free carnitine back out of the matrix where it can be utilized by CPT1.

Acetyl CoA generated from either pyruvate or fatty acid oxidation enters the TCA cycle and combines with oxaloacetate to generate citrate. Citrate is a 6 carbon intermediate that can be oxidized using the tricarboxylic acid (TCA) cycle to produce reduced high energy carriers, nicotinamide adenine dinucleotide (NADH) and Flavin adenine dinucleotide ($FADH_2$). These reduced intermediates are then oxidized to NAD^+ and FAD respectively, and donate electrons to the electron transport chain (ETC, also called mitochondrial respiratory chain) in the inner mitochondrial membrane. The oxidation of NADH and $FADH_2$ donates electrons to complexes I and II of the ETC and electrons are passed down an electronegativity gradient to the final electron acceptor, molecular oxygen, which is quickly converted into water. This consumption of oxygen is commonly referred to as mitochondrial respiration and can be measured directly to investigate ETC function[12]. As electrons are transferred, members of the electron transport chain pump protons from the mitochondrial matrix into the intermembrane space building up a proton gradient. This proton gradient generates mitochondrial membrane potential and is the proton motive force which drives ATP synthesis coupling nutrient oxidation to ADP phosphorylation (Illustration 3).

Oxidative phosphorylation can be circumvented by proton leak in which protons pass down the gradient independent of ATP production resulting in energy lost as heat (thermogenesis). Proton leak lowers mitochondrial membrane potential which leads to an increase in ETC flux and mitochondrial respiration in effort to restore the gradient. This uncoupled respiration is no longer linked to ATP phosphorylation thus to maintain the same levels of ATP, cells must oxidize more nutrients and energy expenditure is

increased. The physiological role of uncoupled respiration is best understood in temperature regulation. Environmental temperatures below an organism's thermoneutral point induce thermogenic mechanisms in which fat stores are oxidized to produce heat by uncoupled respiration[13]. Proton leak can also be induced by chemical uncouplers like 2-4-dinitrophenol (DNP) leading to increased energy expenditure[14]. This mechanism has been linked to weight loss since the 1930s when DNP was approved by the FDA as a weight loss therapeutic; however, the drug proved to have a relatively narrow therapeutic window with fatal consequences and was subsequently removed from the market. This led to research focused on understanding uncoupling proteins, the endogenous mediators of induced thermogenesis, and the effects these proteins have on systemic metabolic regulation.

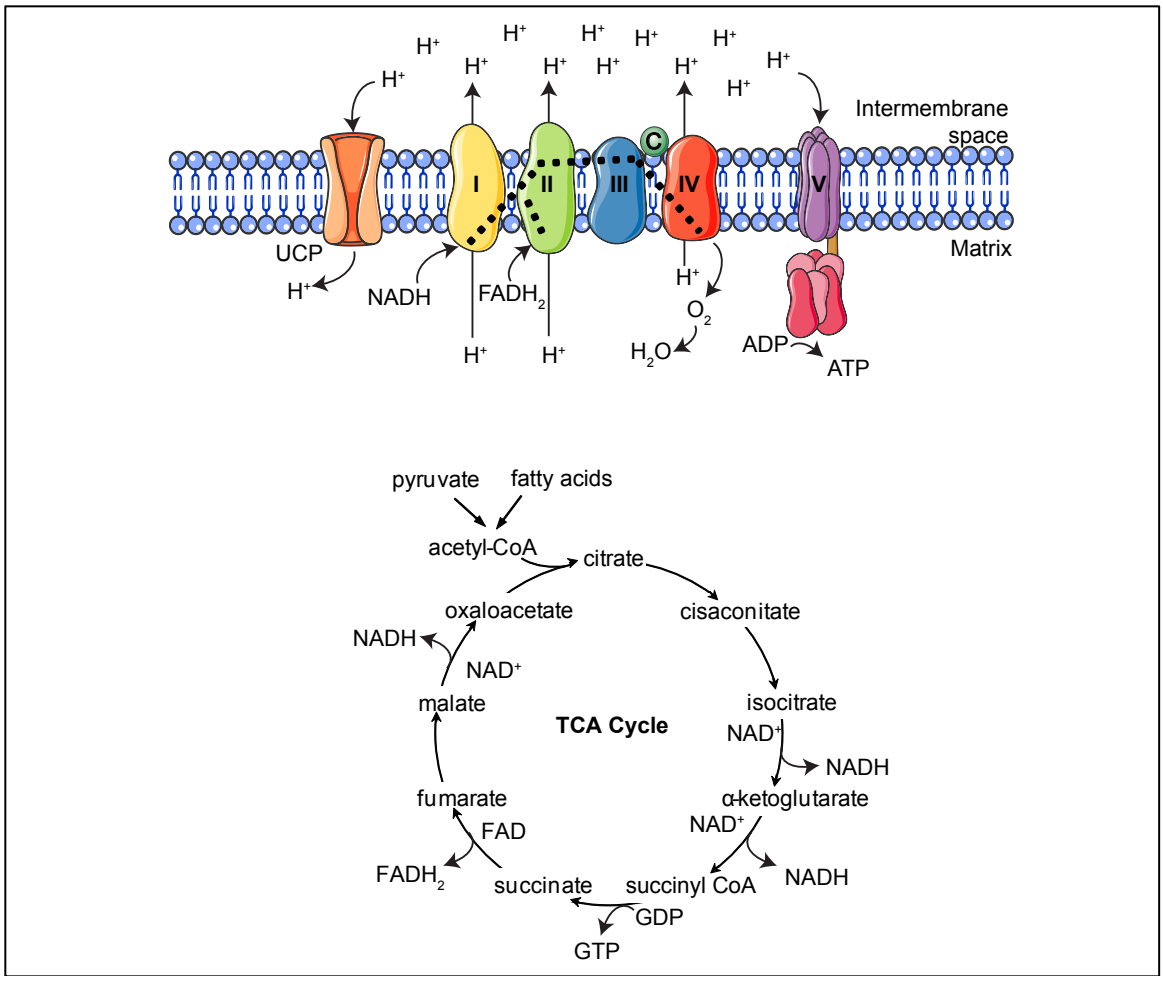

Illustration 3. Mitochondrial TCA cycle and electron transport chain

Acetyl CoA generated from pyruvate or fatty acid oxidation enters the TCA cycle by condensing with oxaloacetate to form citrate. The oxidation of citrate in the TCA cycle regenerates oxaloacetate and generates NADH and $FADH_2$ in the mitochondrial matrix. NADH and $FADH_2$ are then oxidized and donate electrons to the electron transport chain at complexes I and II. Electrons are passed down an electronegativity gradient which allows complexes of the electron chain to transport protons from the mitochondrial matrix into the intermembrane space, building up a proton gradient. This proton gradient makes up mitochondrial membrane potential and is the proton motive force that drives ATP synthesis by complex V. Proton leak can be induced by uncoupling proteins (UCP) which dissipate the proton gradient, lowering mitochondrial membrane potential and increasing mitochondrial respiration uncoupled from ATP synthesis.

1.3 UNCOUPLING PROTEINS AND BODY WEIGHT

Uncoupling proteins (UCPs) are nuclear encoded, transmembrane proteins that localize to the inner mitochondrial membrane and are thought regulate energy expenditure and body temperature by influencing the mitochondrial proton gradient. Within the larger family of mitochondrial solute carrier proteins (SLC25a) there are 5 proteins that make up the uncoupling protein family (UCP1-5)[15]. Uncoupling Protein 1 (UCP1) is considered the prototypical UCP as it was discovered first and is considered the only UCP to function as a protonophore (Table 1). UCP1 is expressed in brown adipocytes and in a recently discovered population of white adipocytes which have a thermogenic capacity (beige or brown adipocytes)[16,17]. UCP1 expression is crucial for mammalian temperature regulation by brown adipose tissue (BAT) and its expression is required for maximal fat oxidation in BAT during times of thermogenic stress. In this way, UCP1 regulates fat storage with relationship to environmental temperatures and limits fat accumulation in animals housed at temperatures below thermoneutrality (30°C)[18].

The relationship between UCP1 and energy expenditure in BAT and beige adipocytes has led many researchers to focus on UCP1 as a therapeutic target for obesity, however studies in humans have shown that BAT mass is inversely proportional to body weight, and beige adipocytes are present in very low numbers, effectively limiting the potential increase in energy expenditure that can be achieved by targeting endogenous UCP1 in obese individuals[16,17,19].

After the discovery of UCP1, two novel uncoupling proteins were discovered (UCP2 and UCP3) which led to great interest in the function of these homologs and their

relationship to thermogenesis and whole body metabolism[20,21]. UCP2 is expressed in many tissues including pancreas, lung, spleen, white adipose tissue and liver while UCP3 expression is confined to skeletal muscle, BAT, heart and skin[22-25]. Although much effort was extended to demonstrate that UCP2 and UCP3 could transport protons like UCP1, this does not seem to be the actual function of these novel UCPs and currently they are hypothesized to transport metabolites involved in TCA cycle function[26,27].

Despite the exact molecular function for UCP2 and UCP3 not being known, a clear link has been established between UCP2/3 function and whole body metabolism in humans through mutational and single nucleotide polymorphism (SNP) analysis[28-34]. UCP2 and UCP3 genes lie within 7kb of one another on chromosome 11 and that genomic region has been suggested to be a quantitative trait loci for body weight in humans[35]. Although UCP2 does play a role in regulating systemic metabolism through regulation of insulin secretion in pancreas along with other tissue specific effects[26,36], the focus of our studies has been on the role that UCP3 plays in influencing systemic metabolism.

	UCP1	UCP2	UCP3	UCP4/5
Expression	BAT beige adipocytes	Pancreas Lung Spleen WAT Liver	Skeletal muscle BAT Heart Skin	Brain CNS tissues
Homology to UCP1	-	56%	57%	34%
Functions	Proton transport Thermogenesis	Aspartate transport Insulin secretion Redox regulation	Malate transport Thermogenesis Fatty acid oxidation	Succinate transport Neurotransmission Mitochondrial biogenesis

Table 1: Uncoupling protein expression and functions

Tissue specific expression of uncoupling proteins likely reflect specialized functions in transport and regulating mitochondrial function. Direct proton transport is fundamental to thermogenesis and has only been observed with UCP1 in thermogenic tissues. There is good evidence that UCP2 controls aspartate transport into the mitochondrial matrix resulting in reduced TCA cycle flux which can alter cellular response such as insulin secretion in pancreatic tissues[26]. UCP3 is alternatively expressed in tissues which undergo lipid oxidation and is thought to support increased TCA cycle flux by importing malate.

The finding that UCP3 is expressed in BAT and skeletal muscle led to initial hypotheses that this protein could be involved in thermogenesis and whole body metabolism however Ucp3 knockout mice display no basal metabolic phenotype[37]. In response to cold exposure, Ucp3 ablation has no effect on core body temperature suggesting that it is not essential for cold-induced thermogenesis since compensatory mechanisms are likely to occur[38]. Similarly, Ucp3 knockout mice are not obese but some evidence still points towards UCP3 regulation of systemic metabolism although the complete mechanisms are not well understood. A comprehensive study of whole body metabolism in UCP3 heterozygous (*Ucp3*$^{+/-}$) and homozygous (*Ucp3*$^{-/-}$) knockout mice with *Ucp3*$^{+/+}$ mice as control demonstrated no difference in body weight among the three genotypes however both *Ucp3*$^{-/+}$ and *Ucp3*$^{-/-}$ mice have increased fasting blood glucose and insulin levels compared with *Ucp3*$^{+/+}$ mice[39]. When mice were fed a high fat diet for 5 weeks, blood glucose levels were no longer increased but *Ucp3*$^{-/-}$ mice displayed significantly increased serum free fatty acid and insulin levels[39]. These data indicate that UCP3 levels influence glucose homeostasis through a mechanism that is influenced by dietary fat intake. In support of this, studies of long term high fat feeding (4-8 months) in *Ucp3*$^{-/-,}$ wild type and UCP3 skeletal muscle specific transgenic mice (UCP3-tg) have reported *Ucp3*$^{-/-}$ mice accumulate more body fat than wild type animals while UCP3-tg mice have reduced body fat compared with wild type[40]. Additionally, UCP3-tg mice have reduced body weights; displays reduced fasting glucose and insulin levels, and are resistant to obesity and insulin resistance with high fat feeding[40,41]. This data clearly

indicates a relationship between UCP3 expression and regulation of glucose-insulin homeostasis and adiposity.

Most of what is known about UCP3 function has been determined from studies in skeletal muscle where UCP3 is induced in response to myoblast differentiation, thyroid hormone and cold exposure as well as fasting and high fat feeding[42,43]. Although there is no evidence that UCP3 directly transports protons in skeletal muscle, mitochondria from *Ucp3*$^{-/-}$ mice have lower levels of uncoupled respiration and fat oxidation compared with wild type mice, suggesting that UCP3 may function similarly to how UCP1 directs fat oxidation in BAT[38]. Additionally, UCP3 function in skeletal muscle is similar to UCP1 in BAT in its ability to lower reactive oxygen species generation and mitochondrial membrane potential[39,44-46]. Finally, both homologs are activated by free fatty acids and inhibited by purine nucleotides indicating that there are conserved aspects of UCP1 and UCP3 function despite the lack of proton transport by UCP3[27].

Consistent with this, mice overexpressing UCP1 in white adipose tissue (WAT) or skeletal muscle are protected from diet-induced obesity suggesting a common mechanism shared by UCP3 and UCP1[8,47,48]. These studies indicate that uncoupling proteins increase the energy expenditure of the tissue in which they are overexpressed and therefore it is somewhat unsurprising that alterations to primary metabolic tissues by uncoupled respiration would influence whole body metabolism. UCP3 expression in skin however has not been evaluated in this capacity and the focus of our studies was to determine if overexpression of UCP3 outside of primary metabolic tissues could have similar protective effects towards body weight and systemic metabolism.

1.4 Skin Biology and Metabolism

Skin is a large organ that prevents water loss and provides essential protection from the external environment. Whole skin is divided primarily into 2 layers: the dermis or lower layer contains sebaceous glands, vasculature, immune cells and substantial extracellular matrix material like collagen for structure and support, and the upper layer or epidermis contains mostly keratinocytes that undergo extensive differentiation to form a stratified epithelial layer and the epidermal lipid barrier. The discussion below will focus primarily on the epidermal layer and metabolic profiles of keratinocytes which function reciprocally with systemic whole body metabolism.

The epidermis is separated from the dermis by a basement layer made up of basal keratinocytes with tight junctions between cells. These cells are generally proliferative and serve as a source for new cells to replace terminally differentiated anucleated corneocytes which are sluffed away. Keratinocytes undergo differentiation which consists of extensive protein synthesis for formation of keratin fibers and lipid synthesis for formation of lamellar bodies, which are secreted by the granular layer to form the epidermal lipid barrier. Basal cells undergoing differentiation will move up from the stratum basal into the stratum spinosum where proper synthesis of lamellar bodies and keratin fibers is essential for healthy skin. From there, cells migrate up in the tissue and enter the granular layer (stratum granulosum) where keratohyalin granuals appear, cells dehydrate and lose their nuclei and organelles and secrete lamellar bodies. Finally, cells migrate into the cornified layer containing dead cells, surrounded by a cornified envelop with extensive lipid networks filling the extracellular space. This process of keratinocyte

proliferation and differentiation is regulated by an endogenous calcium gradient *in vivo* which can be mimicked in cell culture to induce differentiation[49,50].

The basal epidermis contains the most metabolically active cells in skin and since differentiation leads to loss of mitochondria, these cells are primarily responsible for mitochondrial oxygen consumption by epidermis. That being said, the overall respiration rate is low in whole epidermis compared with other tissues, as differentiated keratinocytes primarily utilize glycolysis for ATP production[51,52]. Previous studies have reported a respiratory quotient in epidermis close to 0.7 which should indicate that fatty acids are a predominant source of energy for mitochondrial ATP production[51]. This finding is curious since the majority of metabolic activity in skin is devoted to lipid synthesis, and a high rate of lipid oxidation would likely be futile toward overall tissue homeostasis.

Epidermis represents a major site of *de novo* lipid synthesis that rivals rates of lipid synthesis in both liver and adipose tissue when compared by tissue mass[53]. Lipogenesis is a critical component of skin function and disruption of the epidermal lipid barrier can lead to trans-epidermal water loss and dehydration[49]. Barrier disruption also leads to an increase in cell differentiation and proliferation suggesting that keratinocytes respond to changes in epidermal lipid levels[54]. Lipid synthesis in epidermis utilizes circulating glucose as a carbon source and is stimulated in response to glucose ingestion and inhibited during starvation[55]. During active epidermal lipid synthesis, glucose is taken up and oxidized to acetyl CoA and incorporated into the citrate pool in the mitochondria. Citrate is then exported by mitochondria and converted to cytoplasmic

acetyl CoA that is used as the primary source of carbon to make lipids, similar to lipid synthesis in liver and adipose tissue[56]. Efficient lipogenesis therefore requires glucose and functional mitochondrial enzymes which indicates that basal keratinocytes represent the primary site of de novo lipid synthesis.

Many early studies have indicated nutrition state can regulate epidermal lipid synthesis however, recently it was demonstrated that epidermis may have a reciprocal effect on systemic glucose metabolism. Mice lacking the fatty acid synthesis enzyme steroyl CoA desaturase 1 (SCD1) specifically in basal epidermis have improved glucose tolerance and resistance to high fat diet induced obesity[57]. SCD1 catalyzes the rate limiting step in the synthesis of unsaturated fatty acids by converting palmitate and stearate into palmitoleate and oleate respectively[58]. Decreased enzyme expression leads to a marked reduction in sebaceous gland lipids and alterations to skin surface lipids[59]. This finding demonstrates the capacity for alterations in epidermal lipid synthesis to affect systemic glucose metabolism and led to the hypothesis that increased lipid oxidation through UCP3 overexpression in basal epidermis might also alter systemic glucose metabolism.

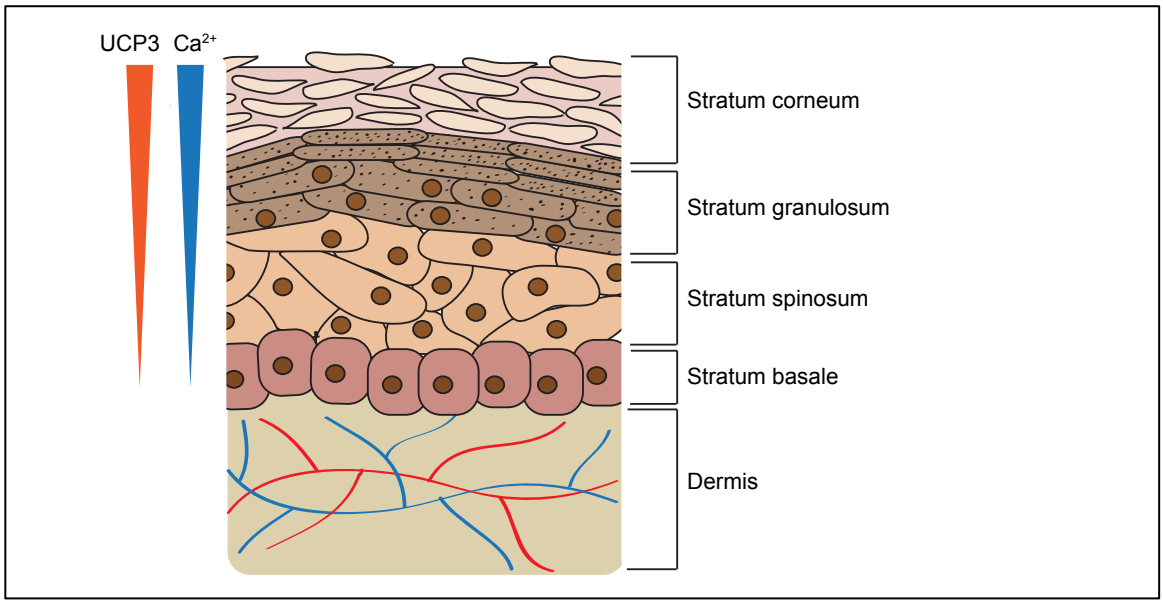

Illustration 4. Cell layers in epidermis

Skin is separated in to dermal (lower) and epidermal (upper) which make up a stratified epithelial barrier from the external environment. The epidermis is regenerated by cells in stratum basal which contains proliferative keratinocytes that can self-renew or undergo differentiation. Upon differentiation, cells migrate into the stratum spinosum and generate keratin filaments and lamellar bodies. From there, cells migrate in to the stratum granulosum and begin to flatten out as keratohyalin granuals appear. As cells mover from the granular layer into the stratum corneum, lamellar bodies are released and lipids fill in the extracellular space surrounding terminally differentiated corneocytes. This lipid makes up the epidermal lipid barrier to protect against water evaporation from skin. Eventually corneocytes are sloughed off and replaced with cells migrating from lower layers of epidermis. Keratinocyte differentiation is regulated by an *in vivo* calcium gradient and UCP3 expression is increased concomitantly with this calcium gradient[25].

Chapter 2: Uncoupled respiration in skin promotes obesity resistance

2.1 THE K5-UCP3 MOUSE MODEL AND METABOLIC PHENOTYPE

In order to investigate the effects of UCP3 overexpression in basal epidermis, we utilized a mouse model in which murine *Ucp3* expression is driven by the bovine keratin 5 promoter (K5-UCP3). This targets overexpression to basal epidermis and the basal layer of other stratified epithelial tissues. Consistent with previous reports of Keratin 5 promoter activity, we observed transgene expression in other stratified epithelial tissues including, oral cavity, esophagus, forestomach, pancreas, lung, bladder and bile duct[60-62]. Although use of this promoter is commonly used in genetic models for studies in basal epidermis, the bovine keratin 5 promoter has also been used to study carcinogenesis in bladder, pancreas, and gall bladder[63-65]. Our lab has previously demonstrated the degree of UCP3 overexpression in K5-UCP3 basal epidermis, as well as the correct localization of UCP3 protein to mitochondria in basal keratinocytes[25]. Additionally, previous studies confirmed transgene function through increased epidermal respiration and have shown that the increased respiration is solely due to increased lipid oxidation (Figure 1A). Gross phenotypic observations of K5-UCP3 mice included that pups were smaller than wild type littermates and the loss of hair, both phenotypes which seem to become less prominent as the mice age (Figure 1B).

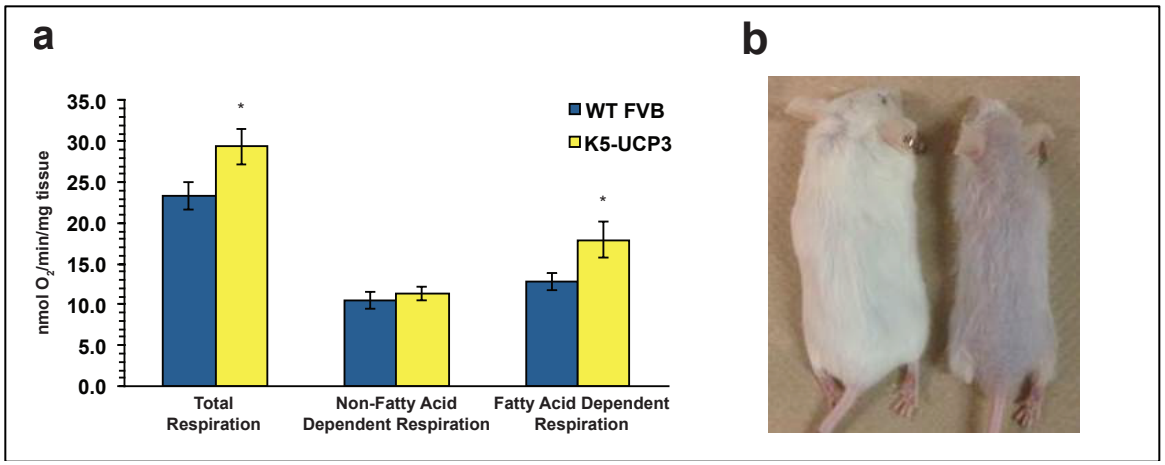

Figure 1. Epidermal respiration due to fatty acid oxidation

(a) *Ex vivo* epidermal respiration due to fatty acids. Whole epidermis was placed in a clark type electrode and oxygen consumption rate was assessed in the presence and absence of Etomoxir (Eto : 40μM) an inhibitor of CPT1 and mitochondrial fatty acid oxidation. Fatty acid dependent respiration was defined as the difference between total respiration and Eto inhibited (fatty acid independent) respiration. Error bars represent mean ± SEM (WT FVB n=10, K5-UCP3 n=8). * Indicates significance from WT FVB/N $p \leq 0.05$.[66] (b) Small and hairless phenotype of K5-UCP3 mice (18 weeks old)

2.1.1 UCP3 overexpression in epidermis prevents obesity due to diet

The small phenotype of K5-UCP3 mice was of particular interest to us and we set out to characterize the changes to systemic metabolism induced by uncoupled respiration in skin. Upon weaning (3-3.5 weeks old, male), transgenic mice weighed on average 20% less than wild type littermates and this reduction in body weight persisted through 6.5 weeks accompanied by an increase in caloric consumption (Figure 2A-B). To further understand the changes in body weight, we performed body composition analysis on young (6-9 weeks, male) and older (15 weeks, male) mice that indicated a significant reduction in both fat and lean mass in young mice with a reduction only in fat mass in older mice (Figure 2C). The reduced fat mass in older mice suggests that as with overexpression in skeletal muscle[67], epidermal UCP3 overexpression can limit fat accumulation. This, taken with the knowledge that UCP3 overexpression drives increased lipid catabolism in skin led to the hypothesis that K5-UCP3 mice would be resistant to high fat diet-induced obesity. To test this, we weaned K5-UCP3 and wild type FVB/N littermates onto a control diet consisting of 10% kcal from fat (Research Diets, D12450) or a high fat diet consisting of 60% kcal from fat (Research Diets, D12492) and measured their body weight and caloric consumption for a period of 15 weeks. The results of our high fat diet study were in agreement with our hypothesis and K5-UCP3 mice were resistant to obesity due to high fat diet (Figure 2D-E). Although both genotypes gained a significant amount of body weight after consuming high fat diet, the K5-UCP3 mice maintained lowered body weights compared with wild type littermates

regardless of diet (Figure 2D-E). There was no difference in the food consumption between genotype (Figure 2F), and body composition analysis revealed K5-UCP3 mice were resistant to fat accumulation seen in FVB/N littermates fed high fat diet. As well, we observed no difference in fat mass between K5-UCP3 mice fed a high fat diet with either genotype fed control diet (Figure 2G). This data indicates that as seen in skeletal muscle[40], UCP3 overexpression in epidermis can limit fat accumulation with obesogenic diet. Collectively these data suggest UCP3 overexpression creates an imbalance in systemic metabolism to limit fat storage and we investigated regulation of glucose and lipid homeostasis to establish specific mechanisms by which phenotype had occurred.

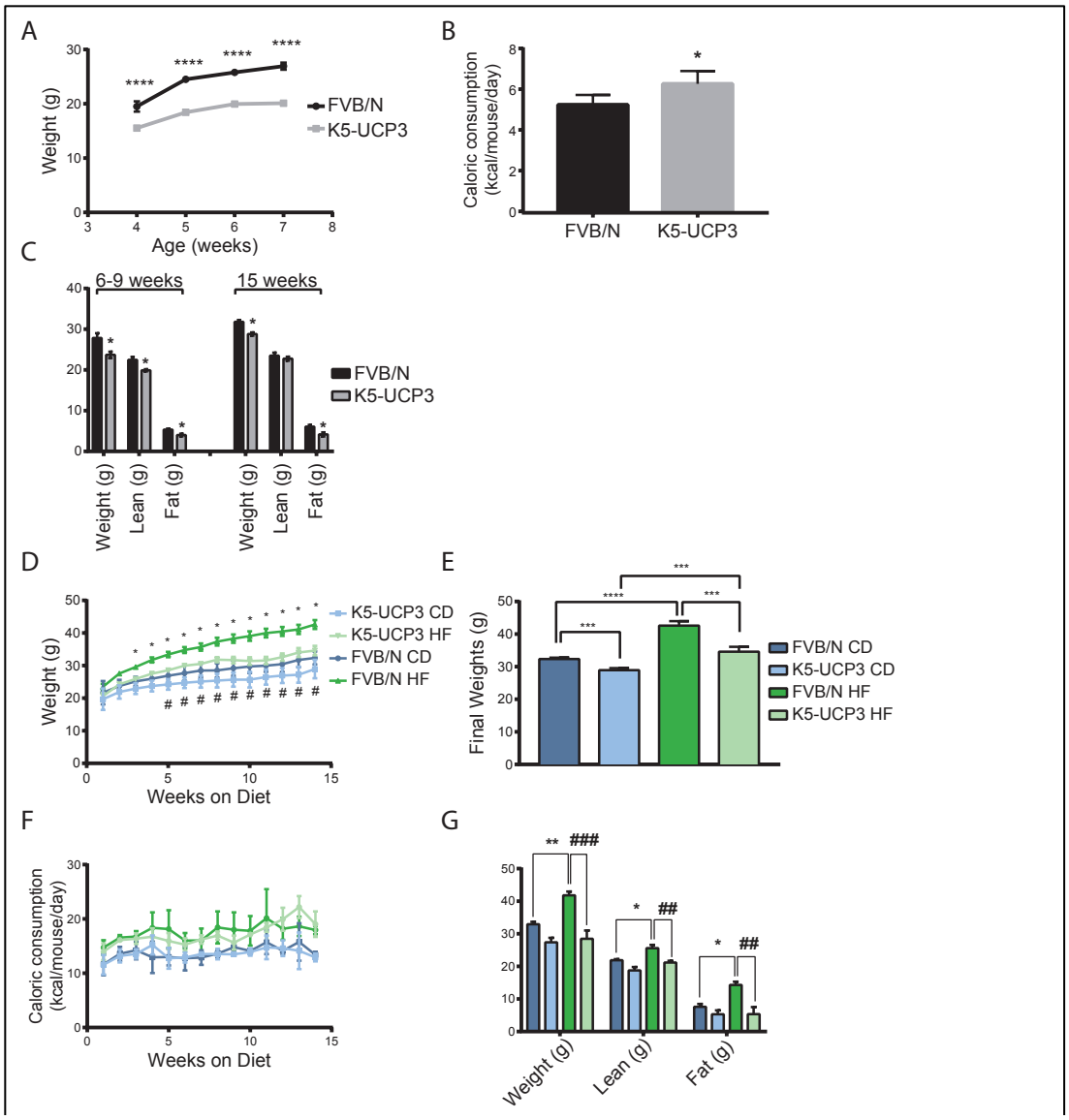

Figure 2. UCP3 overexpression in epidermis reduces body weight and prevents obesity.

(A) Body weight measurements, (B) caloric consumption, and (C) body composition analysis from FVB/N and K5-UCP3 littermates (male, 6 weeks old and 15 weeks old). * indicates significance from FVB/N ($p< 0.05$, ** $p<0.01$, ***$p<0.001$, ****$p<0.0001$). (D) Body weight measurements in FVB/N and K5-UCP3 male littermates fed control (CD) and high fat diet (HF) and (E) final body weights after 15 weeks. (F) Caloric consumption measurements and (G) body composition analysis in FVB/N and K5-UCP3 mice fed control or high fat diet. Error bars are means ± SEM. * indicates significance of FVB/N HF compared with FVB/N CD. # indicates significance of K5-UCP3 HF compared with FVB/N HF.

2.1.2 Uncoupled respiration in skin alters glucose homeostasis

To gain an overall picture of epidermal metabolism in wild type and K5-UCP3 littermates we performed metabolomic analysis on epidermis from 6-9 week old mice (gender matched, N=6) that had been fasted for 5 hours prior to tissue collection to control for feeding differences among mice. Among the multitude of changes to steady state metabolite levels observed between genotypes, markers of increased glucose and lipid catabolism were among the most abundant. (Figure 3A-C) UCP3 overexpression induced a reduction in 6 carbon intermediates at the beginning of the glycolytic pathway and builds up of end products pyruvate and lactate (Figure 3A). We confirmed this increase in glycolysis by measuring increased lactate secretion in primary keratinocytes from wild type and K5-UCP3 epidermis indicating that UCP3 overexpression promotes aerobic glycolysis in a cell autonomous manner (Figure 3D). Importantly, despite data indicating increased glycolysis and fatty acid oxidation in epidermis, primary keratinocytes from transgenic mice contained 20% less ATP than wild type cells indicating that UCP3 overexpression induced nutrient wasting in keratinocytes effectively increasing energy expenditure (Figure 3D).

Consistent with previous studies of UCP3 overexpression in skeletal muscle[39,67], we also observed a significant decrease in circulating blood glucose levels in both fasted and fed K5-UCP3 mice compared with wild type mice (Figure 4A). In addition we observed a modest decrease in fasting insulin levels suggesting that K5-UCP3 mice may be insulin sensitive (Figure 4B).

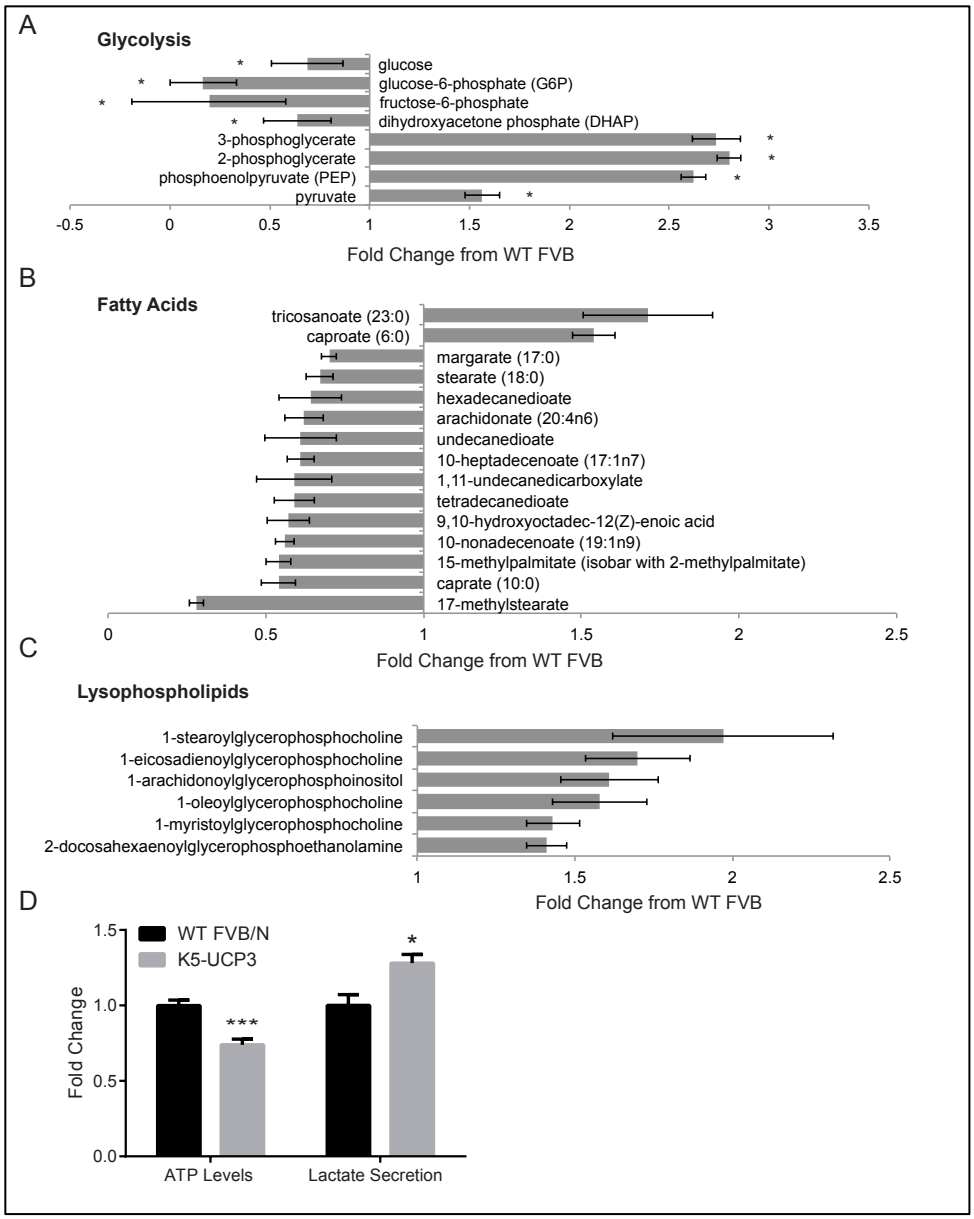

Figure 3. Metabolomics Analysis and ATP levels in K5-UCP3 epidermis.

Metabolomic analysis on 5 hour fasted FVB/N and K5-UCP3 epidermis using LC/MS/MS and GC/MS (Metabolon Inc.) values represent fold change from WT FVB/N for (A) Glycolysis (B) Free Fatty Acids and (C) Lysophospholipids[66]. (D) ATP levels and lactate secretion in isolated primary keratinocytes from FVB/N and K5-UCP3 mice. Values represent fold change from FVB/N. Error bars are means ± SEM. * Indicates significance from WT FVB/N $p \leq 0$.

To further investigate the relationship between increased glycolysis in epidermis and whole body metabolism we performed glucose (GTT) and insulin (ITT) tolerance tests on 6-9 week old wild type and transgenic littermates. Briefly, this consisted of an overnight fast (14-16 hours) and a fasting blood glucose reading taken from the tail, followed by an intraperitoneal (I.P.) injection of glucose (2g/kg) or insulin (0.75U/kg) and regular blood glucose measurements over a period of 3 hours. The GTT is a measure of overall glucose tolerance and the ability of the pancreas to respond to a standard glucose injection by secreting insulin to lower circulating glucose levels. Whereas, the ITT is a measure of the peripheral tissues to respond to a standard insulin injection and take up circulating glucose and inhibition of hepatic glucose production. The results of these tests in K5-UCP3 mice indicated an increase in overall glucose tolerance as determined by a reduction in the area under the curve calculation (AUC) which was due to improved glucose clearance at 30 and 60 minutes post-injection (Figure 4C-D). Insulin sensitivity was not changed between the two genotypes however we did observe a modest reduction in fasting insulin levels in K5-UCP3 mice (Figure 4E, 4A). This data suggests that reduction of blood glucose levels of transgenic mice may be due to an insulin-independent mechanism and may result from increased basal glucose uptake by skin. If basal glucose uptake is increased in the epidermis of K5-UCP3 mice it could consistently reduce blood glucose levels and reduce the amount of circulating insulin necessary to maintain glucose homeostasis.

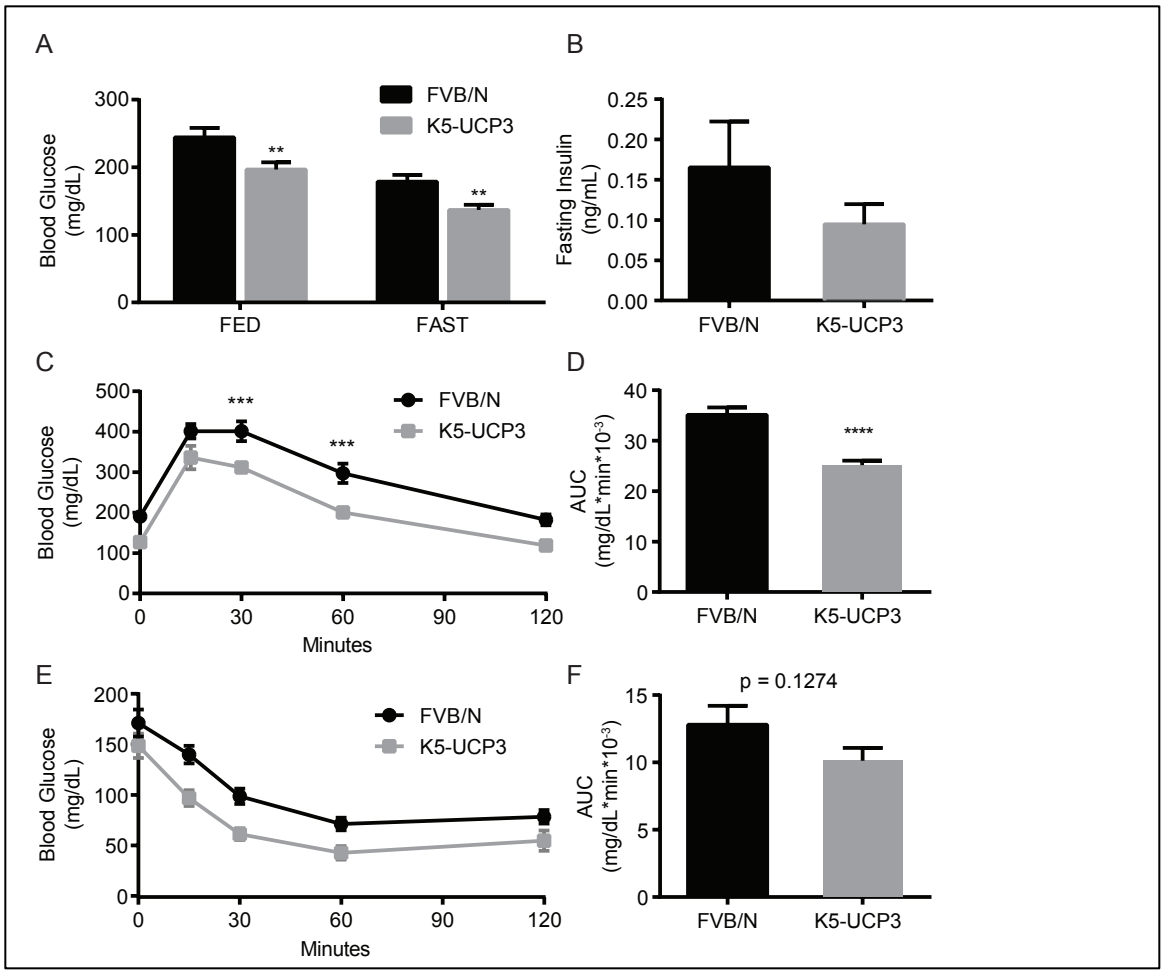

Figure 4. UCP3 overexpression in epidermis alters systemic glucose homeostasis.

(A) Ad libitum fed and 14-16 hour fasting blood glucose levels and (B) fasting insulin levels in FVB/N and K5-UCP3 littermates. (C) Glucose tolerance test with (D) AUC calculation, and (E) Insulin tolerance test with (F) AUC calculations. Error bars are means ± SEM. * indicates significance from FVB/N ($p < 0.05$, ** $p<0.01$, ***$p<0.001$, ****$p<0.0001$)

We investigated the release of energy storage from adipose tissue upon fasting by measuring serum non-esterified fatty acid (NEFA) levels (Figure 5A). These data indicate no difference in serum NEFA between FVB/N and K5-UCP3 littermates suggesting that reduced fat mass did not alter release of energy stores from adipose tissue. Reduced fat mass could lead to alteration in circulating hormones like leptin which can influence liver metabolism. To investigate these questions, we examined metabolic gene expression in liver (which does not express UCP3) under fasted and fed conditions. We observed no difference between genotypes in expression in phosphoenolpyruvate carboxykinase (PEPCK) which is involved in liver gluconeogenesis, pyruvate dehydrogenase kinase 4 (PDK4) which regulates glucose oxidation in mitochondria or CPT1a which regulates fatty acid oxidation in liver (Figure 5B). This led us to conclude that alterations in liver function or circulating hormones were not a causal factor in hypoglycemia induced by UCP3 overexpression in epidermis.

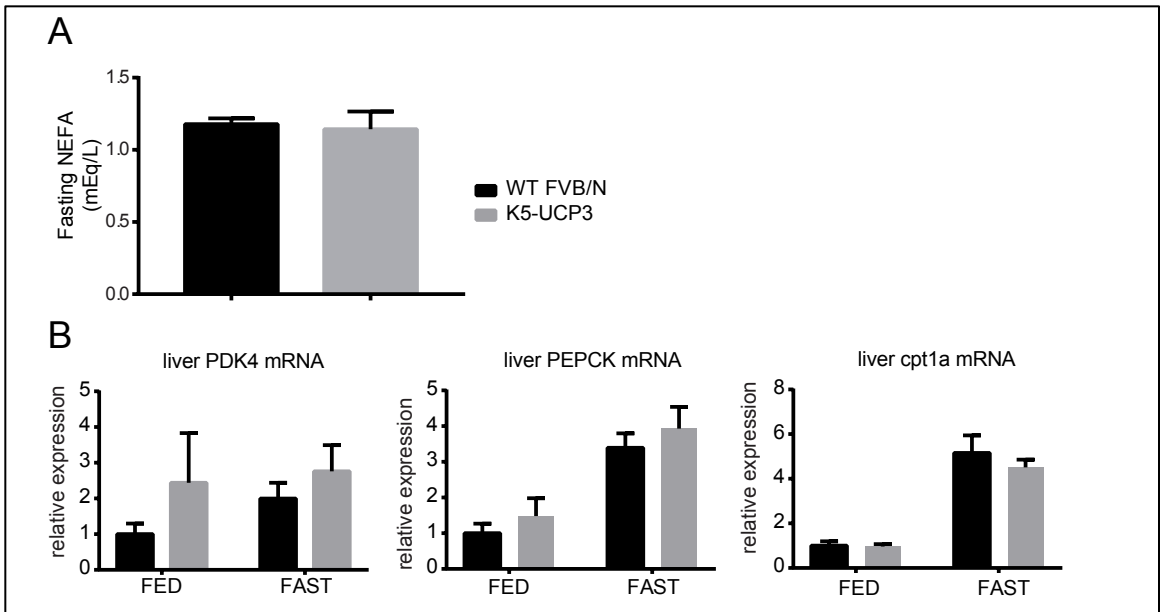

Figure 5. UCP3 overexpression in epidermis does not alter adipose lipolysis or liver metabolism.

(A) Fasting non-esterified fatty acid (NEFA) levels in wild type and K5-UCP3 plasma. (B) Liver mRNA levels of pyruvate dehydrogenase kinase 4 (PDK4), phosphoenolpyruvate carboxykinase (PEPCK) and carnitine palmitoyltransferase 1a (CPT1a) in wild type and K5-UCP3 mice ad lib fed and 14-16 hour fasted. Values represent fold change from FVB/N. Error bars are means ± SEM..

2.1.3 Uncoupled respiration in skin blocks diet-induced metabolic dysfunction

With the knowledge that UCP3 overexpression in skin drives fatty acid oxidation we hypothesized that epidermis might increase glucose uptake in an attempt to replenish lipid levels. Therefore we were interested if increased dietary fat content could rescue the glucose phenotype observed in transgenic mice. Surprisingly, K5-UCP3 mice fed a high fat diet maintained reduced fasting blood glucose levels compared to wild type animals; however, 15 week old mice fed chow or control diet no longer displayed a reduction in fasting glucose which suggests glucose homeostasis in K5-UCP3 mice is altered as mice age (Figure 6A). We also observed significant changes in fasting insulin levels in K5-UCP3 mice on both control and high fat diet (Figure 6B). Despite this, K5-UCP3 mice fed a control diet for 15 weeks showed no difference in glucose or insulin tolerance compared to wild type animals fed the same diet. However, when mice were fed a high fat diet, epidermal UCP3 clearly prevents hyperglycemia, glucose intolerance and insulin resistance (Figure 6C-F). Glucose tolerance tests in high fat fed animals indicated glucose intolerance in wild type mice that was not seen in transgenic mice as indicated by lowered AUC due to reduced fasting blood glucose levels, reduced peak circulating glucose 15 min after injection, and increased glucose clearance 1 hour post-injection (Figure 6C-D). Insulin tolerance tests indicated insulin resistance in wild type animals fed high fat diet as measured by AUC calculations, however transgenic animals fed the same diet exhibited increased glucose clearance at 15 and 30 minutes post-injection (Figure 6E-F). Overall, this data provides a very interesting view of the capacity for

uncoupled respiration in epidermis to influence systemic metabolism and provides further evidence that targeting skin may be a therapeutic option for treating obesity and type 2 diabetes.

2.1.4 Mechanisms opposing obesity in K5-UCP3 mice

The capacity for alterations in skin metabolism to influence systemic metabolism is a viable treatment option only if we understand the specific mechanisms that promote this effect. The experiments presented thus far suggest a model where epidermal UCP3 overexpression induces nutrient wasting, increasing basal glucose uptake in skin which reduces circulating glucose levels and limits fat accumulation. Multiple pieces of data support the finding that UCP3 overexpression induced nutrient wasting in K5-UCP3 mice including: (1) Increased caloric consumption and decreased body weight in young animals (Figure 2A-B) (2) metabolomic analysis indicating global increase in nutrient oxidation of lipids and carbohydrates in transgenic epidermis (Figure 3A-C), (3) tissue respiration rates reveal increased uncoupled respiration and increased mitochondrial fat oxidation in K5-UCP3 epidermis (Figure 1A), and (5) increased lactate secretion but reduced ATP levels in primary keratinocytes from transgenic mice (Figure 3D).

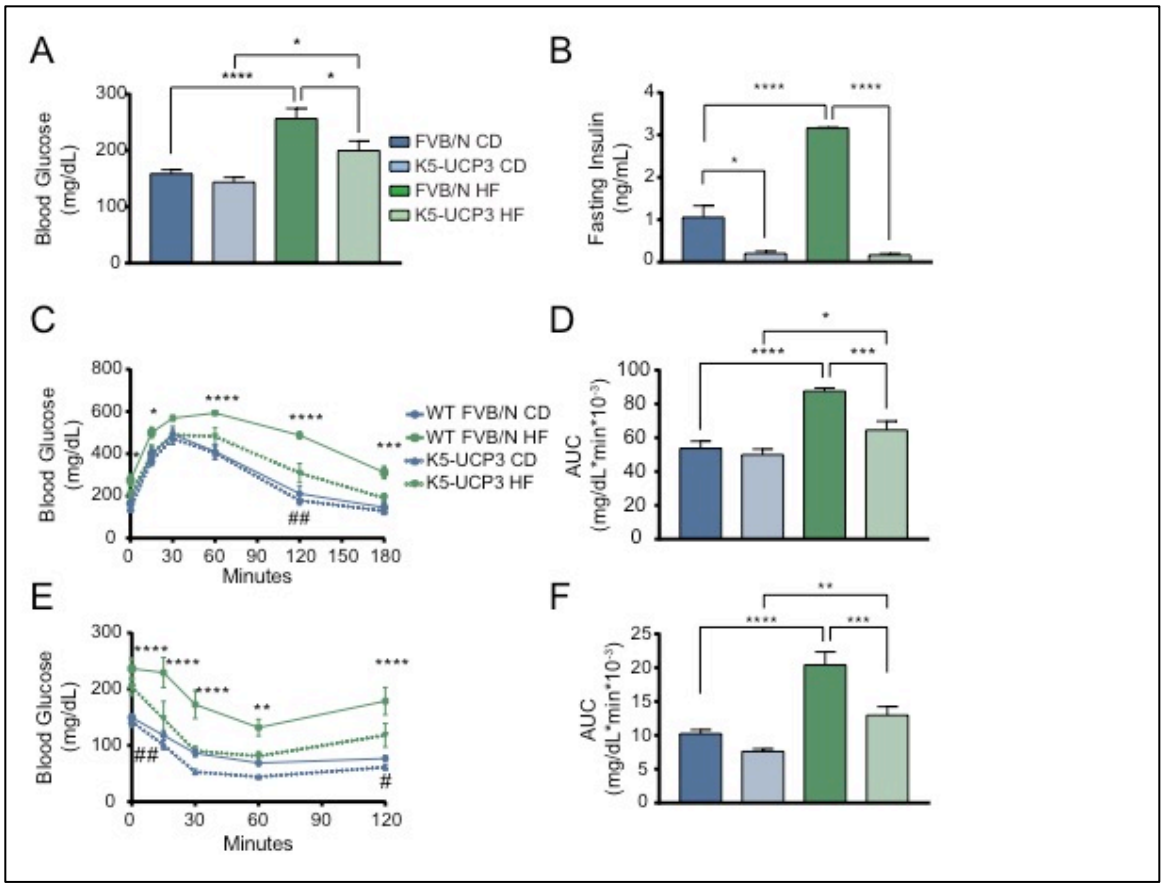

Figure 6. UCP3 overexpression in epidermis prevents diet-induced hyperglycemia and insulin resistance.

(A) Fasting blood glucose levels and (B) fasting insulin levels in 18 week old FVB/N and K5-UCP3 littermates fed control and high fat diet. (C) Glucose tolerance test with (D) AUC calculation, and (E) Insulin tolerance test with (F) AUC calculations. Error bars are means ± SEM. * indicates significance between FVB/N HF compared with FVB/N CD ($p < 0.05$, ** $p<0.01$, ***$p<0.001$, ****$p<0.0001$) # indicates significance of K5-UCP3 HF compared with FVB/N HF

To confirm that basal glucose uptake is enhanced in K5-UCP3 mice we measured expression of glucose transport proteins in wild type and transgenic epidermis (Figure 7A). Previous studies have demonstrated that keratinocytes express glut1, 2, 3, and 5 which are differentially regulated in response to differentiation as well as insulin and IGF-1[68]. Calcium induced keratinocyte differentiation specifically upregulates expression of Glut3, which has higher efficiency than other transporters and higher affinity towards glucose, and downregulates expression of glut1, 2, and 5. Additionally, insulin stimulation increases translocation of Glut 1 and 5 while IGF stimulation induces translocation of Glut 2 and 3 although neither stimulation results in increased glucose uptake by keratinocytes demonstrating that Glut translocation in epidermis is not involved in insulin-stimulated glucose clearance[68]. Consistent with our hypothesis that UCP3 overexpression increases basal glucose uptake in epidermis, we observed induction of glut 1 and glut 3 mRNA in K5-UCP3 epidermis compared with FVB/N littermates in both the fasted and fed state and confirmed these results in fed mice by western blot analysis (Figure 7B). The induction of glut 3 mRNA was not significant and protein levels were only slightly increased suggesting its increase may be associated with increased differentiation markers observed in transgenic epidermis. Importantly, there was no change in *glut1* or *glut3* transcripts with fasting versus feeding in either genotype suggesting that transporter expression is not related to physiological changes in nutrient availability (Figure 7A). In support of our hypothesis that increased glucose uptake in skin is a mechanism that opposes obesity, Glut1 protein remained increased in K5-UCP3 epidermis with both control and high fat diet compared to FVB/N littermates (Figure 7C),

whereas Glut 3 protein was not altered by genotype or diet (data not shown). This data suggests that increased Glut1 expression in epidermis is critical to the mechanism opposing hyperglycemia due to diet in K5-UCP3 mice.

We sought to understand the molecular mechanisms leading to increased glucose transporter expression in epidermis and focused on the role of AMP-activated kinase (AMPK) activation due to its established relationship with both uncoupling and glucose transporter regulation in skeletal muscle. Western blot analysis indicated activation of AMPK in transgenic epidermis as indicated by phosphorylation of threonine 172 (T172) along with phosphorylation and inhibition of its downstream target, ACC at serine 79 (S79) (Figure 7B). AMPK activation and ACC inhibition was maintained in the epidermis of transgenic mice fed both control and high fat diet allowing us to conclude that AMPK activation and ACC inhibition are key factors contributing to mechanism by which UCP3 overexpression in epidermis attenuates fat accumulation and obesity (Figure 7C). Increased AMPK activation and ACC phosphorylation indicates inhibition of epidermal *de novo* lipid synthesis[69] and simultaneously provides a mechanism for increased fatty acid oxidation in K5-UCP3 epidermis through reduced cytoplasmic malonyl CoA levels. Inhibition of ACC and lipid synthesis may mimic some changes to systemic metabolism seen in skin specific *SCD1*$^{-/-}$ mice suggesting that blocking lipid synthesis in epidermis is sufficient to lower circulating glucose levels[70]. The effect of skin *SCD1* knockout on glucose metabolism is rescued by high fat feeding however which indicates UCP3 overexpression promotes changes to glucose metabolism through an alternative mechanism, likely AMPK activation and increased glucose transporter

expression. Future studies distinguishing the effects of AMPK activation and inhibition of lipid synthesis on glucose transporter expression in epidermis would provide critical details necessary for targeting this pathway to limit the development of insulin resistance and type 2 diabetes.

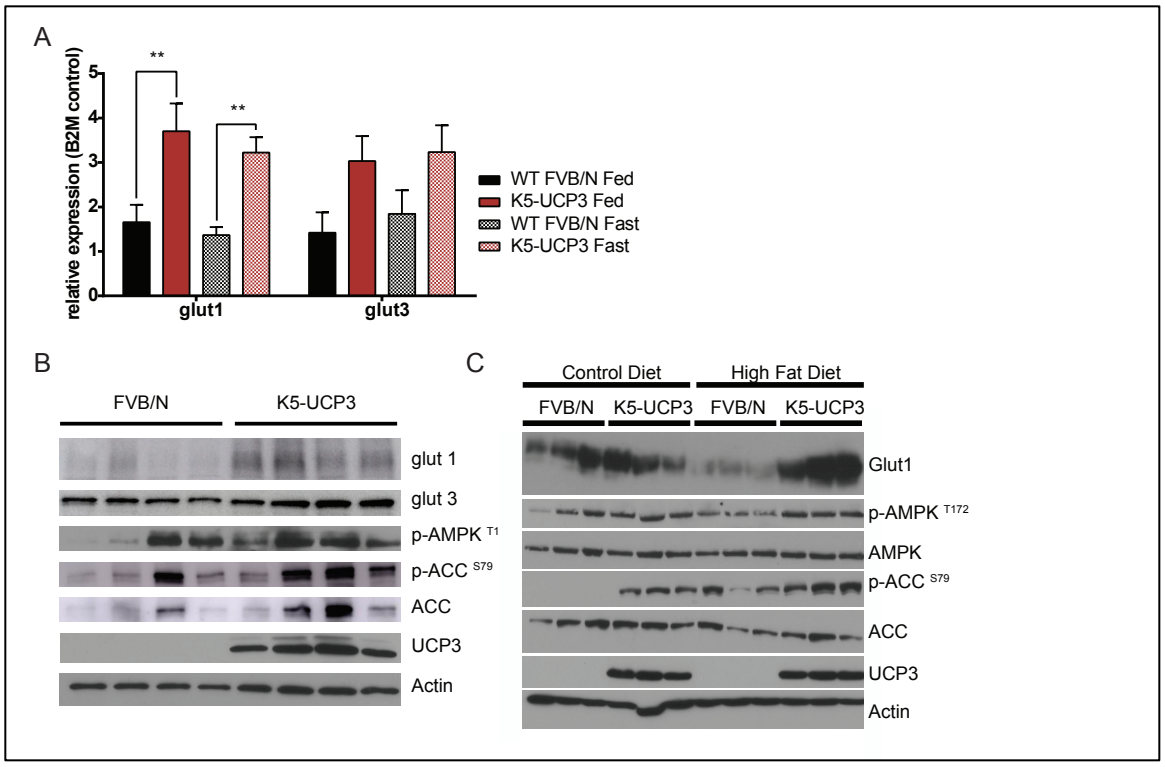

Figure 7. Mechanisms opposing obesity in epidermis of K5-UCP3 mice.

(A) mRNA levels for glut1 and glut3 normalized to B2M control gene in FVB/N and K5-UCP3 fasted (14-16 hours) and fed epidermis. (B) Immunoblot for glucose transporters (glut1 and glut 3) and AMPK activation by phosphorylation at T172 and downstream inhibition of ACC by phosphorylation at S79. Samples are 4 independent epidermal samples from 6-9 week old ad lib fed mice. (C) Immunoblotting in FVB/N and K5-UCP3 mice fed control or high fat diet for 15 weeks. Samples are 3 independent epidermal samples from 18 week old, ad lib fed mice.

Chapter 3: Uncoupled respiration in epidermis inhibits tumorigenesis

3.1 Metabolism and Cancer

Within the last several decades our understanding of metabolism has been greatly expanded through studies of metabolism in cancer. Cell growth and proliferation are energetically demanding processes that require effective metabolism of available nutrients along with proper regulation of gene expression and signaling. Oncogenic mutations in metabolic enzymes, signaling proteins and transcription factors can all promote a metabolic switch that supports the high proliferative demands of cancer cells thus interventions that obstruct this metabolic switch can theoretically prevent cancers in many tissues and with varied genotypes[71]. Metabolic reprogramming seen in cancers is largely defined as the increase in aerobic glycolysis and reduced mitochondrial substrate oxidation defined as the Warburg effect. Glycolysis is much less efficient for ATP production compared to oxidative phosphorylation in mitochondria however this switch allows proliferating cells to generate considerable amounts of biomass in the form of nucleotides, amino acids and intermediates for lipid synthesis from glycolytic intermediates[71]. Decreased oxidative phosphorylation in mitochondria also increases the capacity for cells to liberate TCA cycle intermediates like citrate to support *de novo* lipid synthesis which is critical for cancer cell growth since blocking this process can limit

proliferation both *in vitr[1]o* and *in vivo*[72,73]. With this knowledge, we hypothesized that uncoupled respiration could limit both the energy and metabolic intermediates required for biosynthesis in cancer cells effectively limiting their proliferative potential.

3.1.1 UNCOUPLED RESPIRATION REDUCES PROLIFERATION IN RESPONSE TO TPA

Initial studies using K5-UCP3 mice tested the hypothesis that uncoupled respiration is incompatible with cancer cell growth[25]. To address this question *in vivo*, we employed the two stage chemical carcinogenesis model, which mimics multi-stage skin carcinogenesis seen in humans[74]. Briefly, mice were exposed to an initial subcarcinogenic dose of the DNA damaging agent 7,12-Dimethylbenz[a]anthracene (DMBA) followed by a two week washout period and then biweekly treatment with the tumor promoting agent 12-O-tetradecanoylphorbol-13-acetate (TPA). This method induced papilloma formation in wild type animals after 5 weeks of TPA treatment however K5-UCP3 mice showed a 10 week latency in papilloma formation and greatly reduced papilloma multiplicity. Similarly, wild type animals showed papilloma progression to carcinomas after 10-12 weeks of TPA treatment while K5-UCP3 mice were completely resistant to carcinoma formation[25]. To further investigate the mechanisms by which UCP3 overexpression prevents tumorigenesis, we crossed K5-

---

1 Portions of this chapter are adapted from:
Sara M. Nowinski*, **Ashley Solmonson***, Joyce E. Rundhaug, Okkyung Rho, Christine K. Dao, Cory U. Lago , Kaoru Kiguchi, Susan M. Fischer, John Digiovanni, and Edward M. Mills. *Mitochondrial uncoupling links lipid catabolism to inhibition of Akt and cancer resistance*. Nature Communications 6:8137. August 2015. *** These authors contributed equally to this work.**

UCP3 mice with "pre-initiated" mice harboring an oncogenic v-Ha-RAS transgene (Tg.AC mice) in an attempts to distinguish between UCP3-induced effects on tumor initiation and tumor promotion[75]. In this second tumor study, Tg.AC mice and K5-UCP3/Tg.AC mice received 4 treatments of TPA which induced papilloma formation in Tg.AC mice within a 1-2 weeks after TPA treatment however K5-UCP3/Tg.AC showed a 15 week latency in papilloma incidence with significantly reduced papilloma multiplicity (Figure 8A-C). In addition, similar to the initial tumor study, K5-UCP3/Tg.AC mice were completely resistant to carcinoma formation supporting the hypothesis that UCP3 overexpression blocks skin carcinogenesis (Figure 8D-E). The results of this second study indicate that UCP3 overexpression primarily blocks the tumor promotion stage of skin carcinogenesis and further experiments focused on the effects of UCP3 overexpression on keratinocyte proliferation in response to TPA treatment.

We began by measuring DNA synthesis *in vivo* by labeling proliferative cells with 5-bromo-2-deoxyuridine (BrdU) after topical treatment of either vehicle (acetone), single TPA treatment (1x) and multiple TPA treatments (4x) (Figure 8F). Although K5-UCP3 epidermis did display a modest increase in basal keratinocyte proliferation compared to wild type with vehicle treatment, the proliferative response to TPA treatment was severely blunted with just a 1.5 fold increase in proliferation compare with the 7 fold increase seen in wild type epidermis (Figure 8G). Taken with our data of increased differentiation in K5-UCP3 epidermis this data suggests a small increase in basal cell proliferation may compensate for increased keratinocyte turnover in transgenic epidermis

however stimulated proliferation is markedly decreased in response to UCP3 overexpression.

3.3.2 UNCOUPLED RESPIRATION BLOCKS AKT ACTIVATION

To understand the mechanisms responsible for inhibiting proliferation in transgenic epidermis, we investigated signaling events downstream of TPA treatment. K5-UCP3 epidermis also failed to induce cell cycle proteins cyclin A and cyclin D, and maintained expression of cell cycle inhibitory proteins p21 and p27 in response to TPA (Figure 9A). Broad analysis of cell signaling pathways indicated a striking reduction in activation of Akt (protein kinase B) as observed by decreased phosphorylation at both serine 473 (S473) and threonine 308 (T308) (Figure 9B). This corresponded to reductions in phosphorylation of downstream targets of Akt including glycogen synthase kinase-3β (GSK3β-S9), Forkhead box protein O1 (FOXO1 S256, S319) (Figure 9B).

Akt is a serine/threonine protein kinase that is activated in response to mitogens including epidermal growth factor (EGF) through a mechanism that requires membrane localization of Akt and phosphorylation by mammalian target of Rapamycin complex 2 (mTORC2) at S473 and Phosphoinositide-dependent kinase 1 (PDK1) at T308. Active Akt has a relatively broad impact on cellular function by phosphorylating proteins involved in cell cycle progression, cell survival/anti-apoptosis, protein translation, and cellular metabolism. Specifically with regard to cellular metabolism, activation of Akt leads to increased glycolysis, increased lactate production and increased lipogenesis however little is known about if changes cellular metabolism can influence Akt activity.

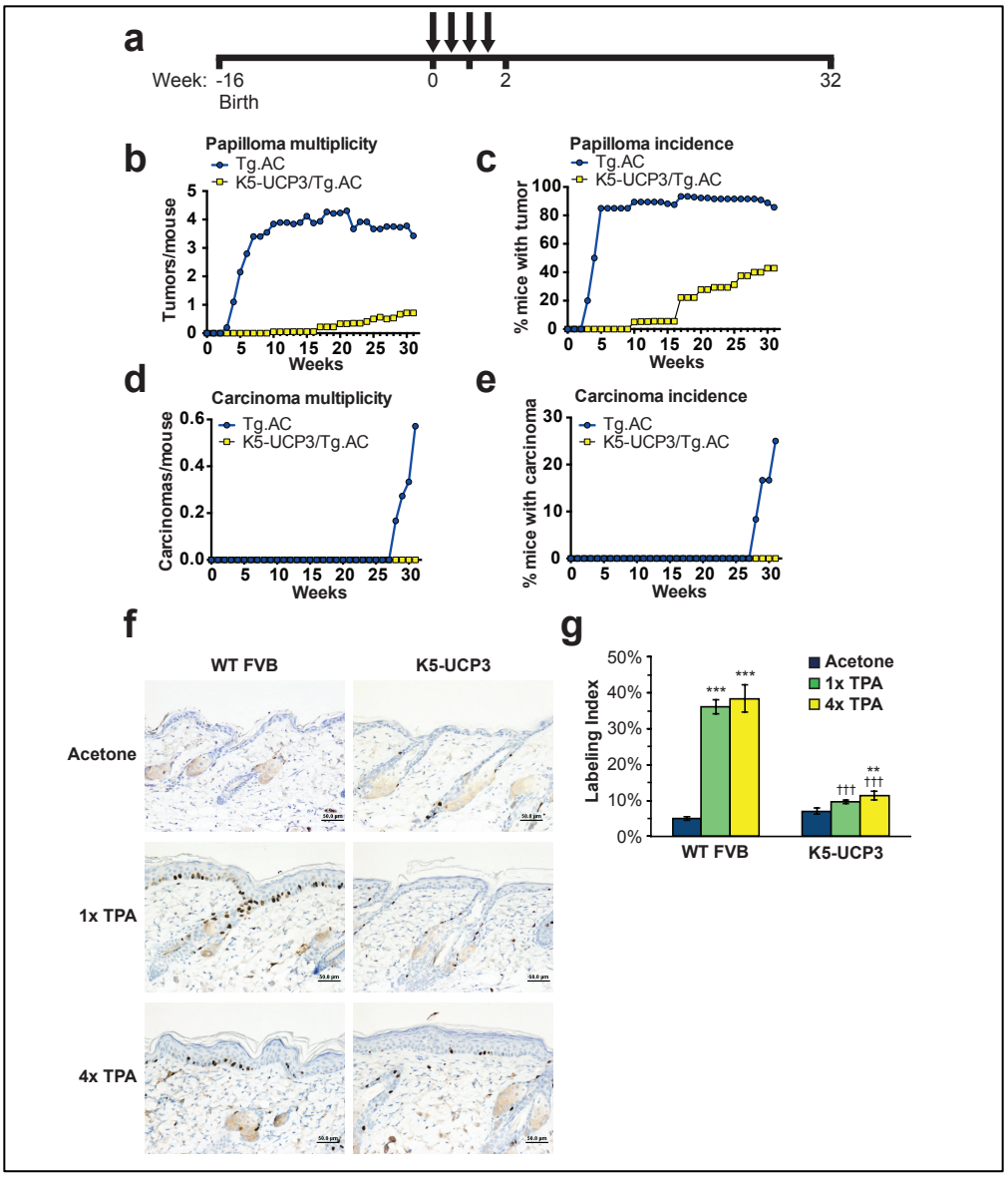

Figure 8. UCP3 blocks tumor promotion

(A) Timeline of Tg.AC tumor study. 16 week-old mice were shaved dorsally and treated topically with TPA biweekly for 2 weeks for a total of 4 treatmets. (B) Tumor development in "pre-initiated" Tg.AC and bigenic K5-UCP3/Tg.AC mice indicating total papillomas/mouse, (C) % mice bearing papillomas, (D) total carcinomas/mouse, and (E) % mice bearing carcinomas. (E) Immunohistochemistry for BrdU labeled cells in wild type FVB and K5-UCP3 epidermis following topical treatment with Acetone (vehicle control), single (1x) or multiple (4x) treatments with 2.5 μg TPA. Scale bars = 50

microns. (F) Quantification of percentage of BrdU-positive labeled cells in the basal layer of the interfollicular epidermis (IFE). Error bars are means +/- SEM. * indicates significantly different from Acetone control, same genotype (** $p<0.01$, *** $p<0.0001$), † indicates significantly different from wild type FVB, same treatment (††† $p<0.0001$).

Furthermore, Akt is central to the phosphatidylinositol 3-kinase (PI3K) – Akt – mTOR signaling pathway which is frequently hyperactive in cancer cells with mutations frequently found in PI3K, PTEN, Akt, TSC2, and mTOR, highlighting the importance of identifying novel mechanisms to inhibit this pathway. Our finding that overexpression of UCP3 inhibits Akt activation was suggestive of a novel mechanism through which targeting metabolism can inhibit proliferation thus we set out to determine the mechanisms by which this inhibition had occurred.

In our analysis of signaling events downstream of Akt, we observed phosphorylation of mTOR at S2448 that was either unchanged of slightly diminished and auto-phosphorylation at S2481 was unaffected. These indicate a maintenance of mTOR activity in TPA-treated K5-UCP3 epidermis despite reduced Akt activation and AMPK activation. This is supported by no difference between transgenic and wild type TPA-treated epidermis in phosphorylation of targets downstream of mTORC2, ribosomal S6, (rS6), eukaryotic translation initiation factor 4E-binding protein 1 (4EBP1) and eukaryotic factor 4G (eIF4G) (Figure 9C). This data, along with activation of AMPK in epidermis suggests that the PI3K-Akt-mTOR pathway may undergo unique metabolic regulation in keratinocytes and certainly warrants further investigation.

To identify if the mechanisms leading to Akt inhibition were cell autonomous, we isolated primary keratinocytes from wild type and transgenic mice and treated these cells with EGF or vehicle (BSA) for 30 minutes (Figure 9D). Akt activation was robust in wild type cells however K5-UCP3 keratinocytes maintained reduced Akt activation indicating that the mechanism was indeed cell autonomous and was not specific to TPA

stimulation as EGF also failed to activate Akt. With the knowledge that EGF stimulation failed to activate Akt in primary cells, we investigated the activation of the EGF receptor (EGFR) in K5-UCP3 primary cells by immunoblot for tyrosine 1086 (Y1086) (Figure 9E). EGFR activation was unaffected by UCP3 overexpression leading us to conclude that blockade of Akt activation occurred downstream of EGFR. Additionally, we demonstrated UCP3-induced inhibition of Akt in human primary neonatal keratinocytes transfected with UCP3, indicating that this mechanism is not specific to murine cells (Figure 9F).

Our data indicated reduced phosphorylation of both S473 and T308 thus we examined the activity of protein phosphatase 2A (PP2A) which is responsible for dephosphorylating both sites to inactivate Akt. The expression of PP2A subunits was not altered by UCP3 overexpression (data not shown), however results of an *in vitro* phosphatase assay indicated that basal PP2A activity was increased in K5-UCP3 epidermis (Figure 9G). This data was in line with decreased activation of another PP2A target, p38-MAPK in transgenic epidermis after TPA treatment however when mice were treated topically with the PP2A inhibitor okadaic acid, p38-MAPK activation was rescued completely whereas Akt activation was only partially rescued (Figure 9H). From this data we concluded that although PP2A hyperactivity played a role in reduced Akt activation in K5-UCP3 epidermis, there was likely an additional mechanism by which UCP3 overexpression could inhibit Akt.

3.3.3 INCREASED β-OXIDATION BLOCKS AKT MEMBRANE RECRUITMENT IN KERATINOCYTES

Downstream of EGFR activation, EGF stimulation activates PI3K to phosphorylate phosphatidylinositol 4,5-bisphosphate (PIP2) to generate phosphatidylinositol (3,4,5)-trisphosphate (PIP3) in cellular membranes. The accumulation of PIP3 provides a docking site for the pleckstrin homology domain (PH domain) of Akt resulting in membrane recruitment and activation of Akt through phosphorylation by upstream kinases mTORC2 and PDK1[76]. We investigated whether UCP3 overexpression affected Akt membrane recruitment in epidermal membranes of acetone and TPA treated mice. Immunoblot for total Akt showed reduced Akt levels in membrane fractions taken from K5-UCP3 mice after TPA treatment compared to wild type littermates indicating that UCP3 overexpression blocks Akt membrane recruitment (Figure 10A-B). The data presented thus far suggest a model where UCP3 overexpression blocks tumor promotion through reduced proliferation resulting from inhibition of Akt membrane recruitment. The localization of UCP3 to the inner mitochondrial membrane suggests an indirect mechanism inhibiting Akt membrane recruitment and thus we focused on our knowledge of UCP3 functional effects on cellular metabolism. Initially, we hypothesized that UCP3 overexpression may decrease cellular reactive oxygen species (ROS) generation which might explain PP2A hyperactivity as well as Akt inhibition. However we were unable to detect any difference in overall cellular ROS or ROS generated by isolated mitochondria from K5-UCP3 epidermis (data not shown). As well, we observed no difference in the redox state of PP2A or Akt (data

not shown) leading us to conclude that UCP3 mediated reduction in ROS was not the mechanism by which Akt inhibition had occurred . Subsequently, we investigated the role of UCP3 induced lipid catabolism as a mechanism to inhibit Akt activation with the use of epidermal metabolomics. Analysis of steady state metabolite levels in K5-UCP3 epidermis indicated global reduction in free fatty acids and acyl-carnitines indicating increased lipid catabolism as a result of uncoupled respiration (Figure 3B). Additionally, uncoupled respiration increased the levels of lysophospholipids indicating increased phospholipid breakdown in K5-UCP3 epidermis and suggesting possible altered membrane composition (Figure 3C). Using this information, we hypothesized that increased lipid catabolism in K5-UCP3 epidermis altered membrane dynamics and reduced the activation potential of Akt at the membrane.

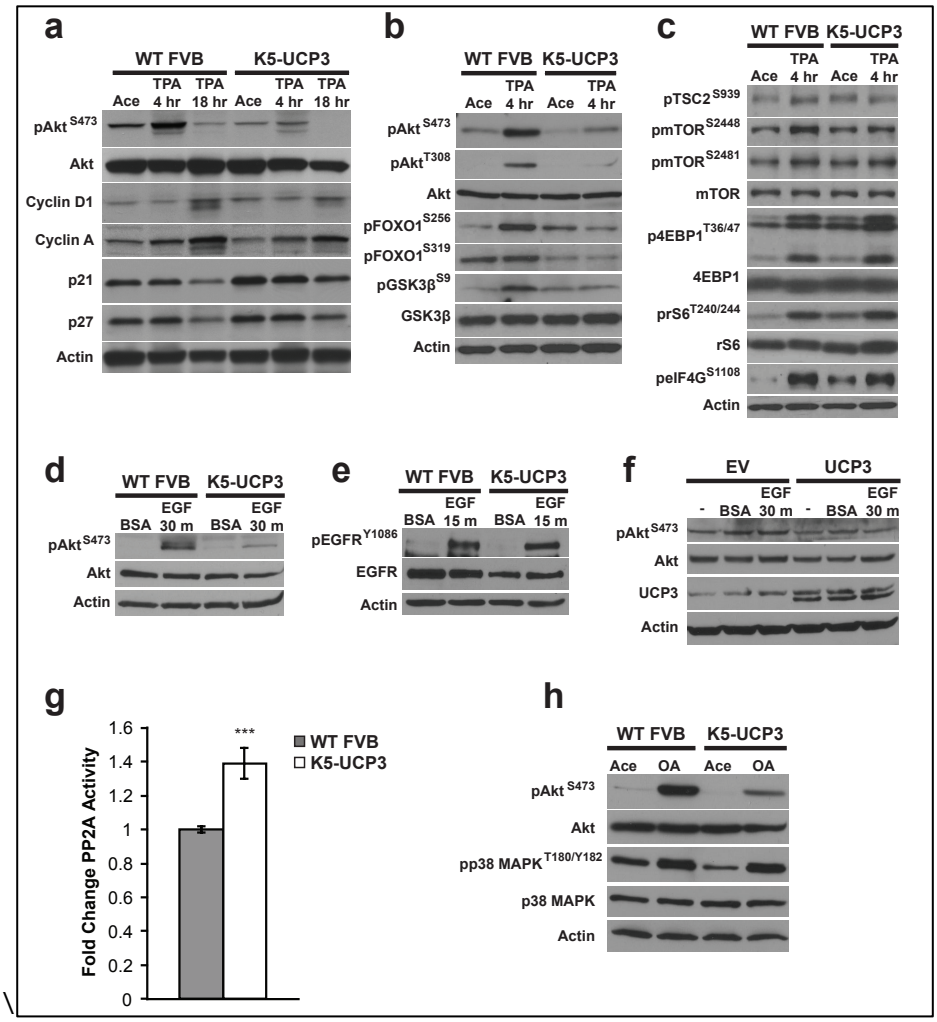

Figure 9. UCP3 overexpression inhibits Akt activation

(A) Immunoblot for Akt phosphorylation at Ser 473, along with total Akt, Cyclin D1 Cyclin A, p21 (Cip1/Waf1) and p27 (Kip1) expression following treatment with Acetone (vehicle control, 4 hours post-treatment) or TPA (4 hours & 18 hours post-treatment) in wild type FVB and K5-UCP3 epidermal lysates. (B) Immunoblot for Akt phosphorylation at Ser 473 and Thr 308, and Akt targets, FOXO1 at Ser 256 and Ser 319, and GSK3β at Ser 9 in wild type FVB and K5-UCP3 epidermal lysates, following treatment with TPA or Acetone. (C) Immunoblot for phosphorylation of mTORC1 pathway members: TSC2 Ser 939, mTOR Ser 2448, Ser 2481, 4EBP1 Thr 36/47, rS6 Thr 240/244, and eIF4G Ser 1108, in wild type FVB and K5-UCP3 epidermal lysates following topical treatment with 2.5 µg TPA or Acetone. (D) Immunoblot for phosphorylation of Akt Ser 473 in serum starved wild type FVB and K5-UCP3 primary epidermal keratinocytes, 30 minutes after treatment with 40 ng/mL EGF or 0.001% BSA

(vehicle control). (E) Immunoblot for phosphorylation of epidermal growth factor receptor (EGFR, Ser 1086) in serum starved wild type FVB and K5-UCP3 primary epidermal keratinocytes 15 minutes after treatment with 40 ng/mL EGF or 0.001% BSA. (F) Immunoblot for phosphorylation of Akt Ser 473 in primary neonatal human keratinocytes transiently transfected with UCP3 or empty vector control (EV) and treated with 40 ng/mL EGF or 0.001% BSA. Immunoblot for UCP3 confirmed successful transfection. (G) *In vitro* PP2A catalytic activity, expressed as fold change compared to wild type. Immunoprecipitated PP2Ac was incubated with a target phosphopeptide and free phosphate release was measured using a malachite green assay and absorbance at 620 nm. Error bars are means +/- SEM. *** indicates significantly different from wild type ($p<0.001$). (H) Immunoblot for Akt Ser 473 and p38 MAPK T180/Y182 phosphorylation in wild type FVB and K5-UCP3 epidermal lysates 1 hour following topical treatment with 5 nmol okadaic acid (OA) or acetone (vehicle control). Immunoblotting for β-Actin was used to confirm equal loading (A-F, H)

To test this hypothesis, we treated wild type and K5-UCP3 mice topically with the CPT1 inhibitor, etomoxir to inhibit mitochondrial fatty acid import and oxidation. Surprisingly, etomoxir not only increased basal Akt activation in transgenic epidermis but also in wild type epidermis indicating that fatty acid oxidation is indeed a novel mechanism to regulate Akt activation (Figure 10C)

3.3.4 OVEREXPRESSION OF AKT RESCUES PROLIFERATION IN K5-UCP3 EPIDERMIS

To confirm that UCP3-mediated lipid oxidation was of functional importance in the tumor resistant phenotype of transgenic mice, we inter-bred K5-UCP3 animals with mice overexpressing a wild type Akt transgene also targeted to basal epidermis (K5-Akt) to generate bi-transgenic mice (K5-UCP3/K5-Akt) [77]. We used these mice to test whether increased expression of Akt could overcome the metabolic regulation of UCP3 in epidermis and rescue cell proliferation and tumorigenesis. K5-Akt mice have been previously reported to have increased Akt expression and basal activation compared to wild type controls and we observed this effect in bi-transgenic mice as well indicating that Akt overexpression was sufficient to overcome inhibition by UCP3 (Figure 11A). Consistent with this, BrdU labeling *in vivo* indicated overexpression of Akt rescued cell proliferation in response to TPA treatment as well as tumorigenesis when subjected to the two-stage chemical carcinogenesis protocol (Figure 11B-C).

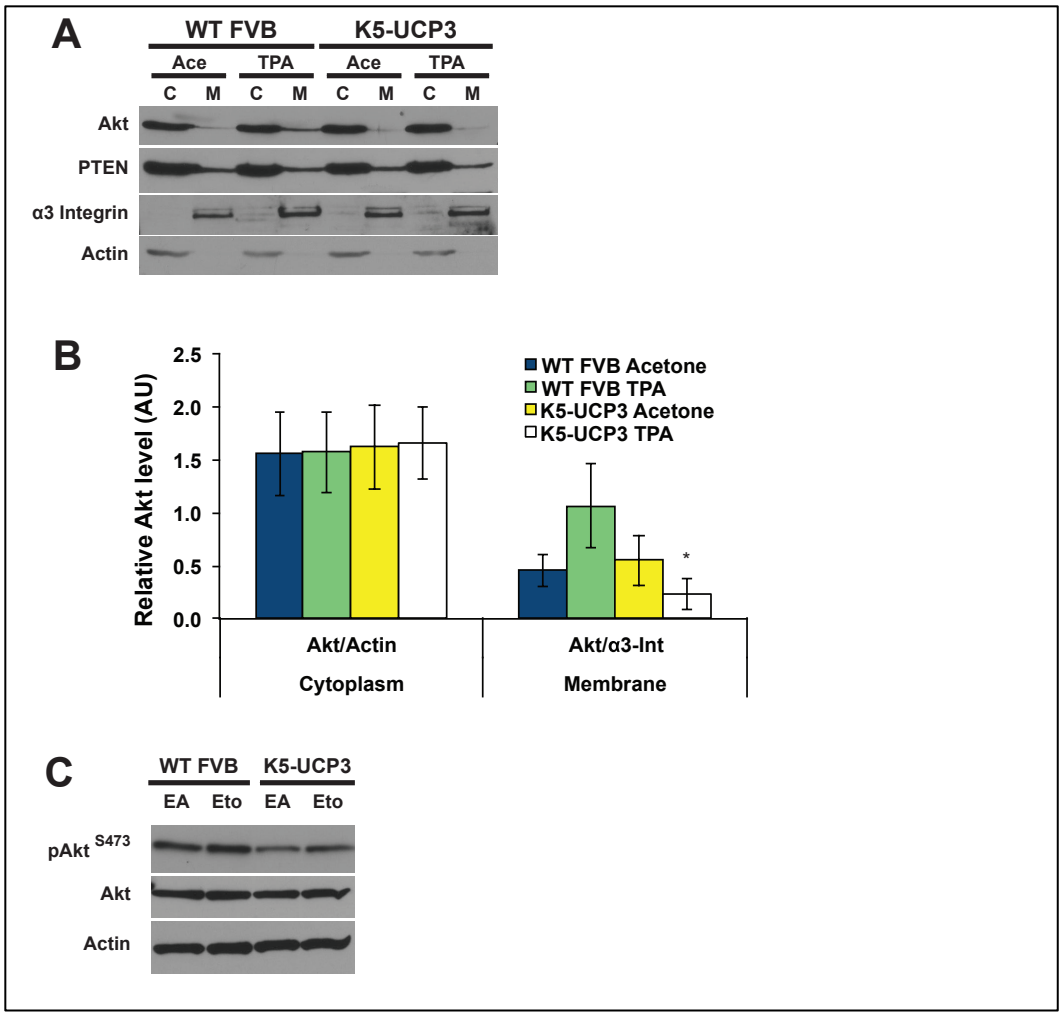

Figure 10. Mitochondrial β-oxidation alters plasma membrane lipids & signaling

(A) Immunoblot for sub-cellular localization of Akt and PTEN in membrane and cytoplasmic fractions from wild type FVB and K5-UCP3 epidermis topically treated with 2.5 μg TPA or Acetone. α-3 Integrin and β-Actin were used as controls to verify membrane and cytoplasmic fractions, respectively. (B) Relative quantification of Akt in cytoplasmic and membrane fractions from triplicate separate immunoblotting experiments via densitometry. Cytoplasmic and membrane fractions were normalized to β-Actin and α3-Integrin, respectively. Error bars are means +/- SEM. * indicates significantly different from wild type FVB, same treatment (* $p<0.05$). (C) Immunoblot for Akt Ser 473 phosphorylation in wild type FVB and K5-UCP3 epidermal lysates 6 hours following topical treatment with 1 mg etomoxir ethyl ester (Eto) or ethyl acetate (EA, vehicle control). Immunoblotting for β-Actin was used to confirm equal loading.

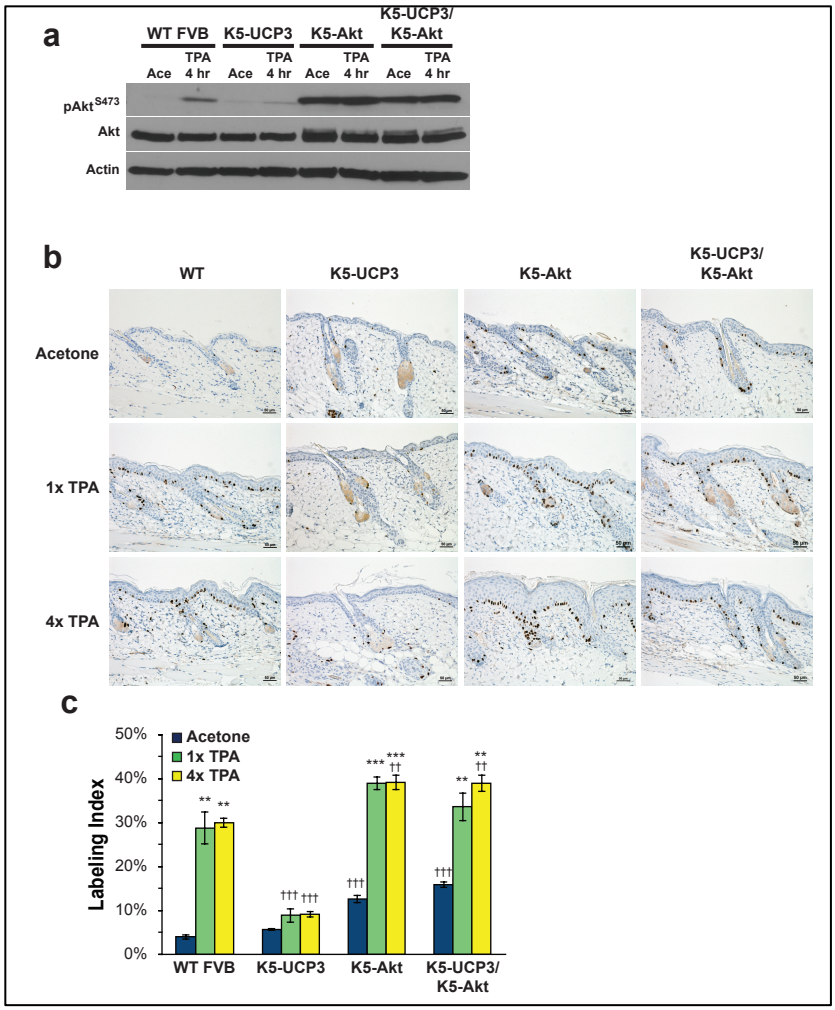

Figure 11. Overexpression of Akt rescues proliferation in K5-UCP3 epidermis

(A) Immunoblot for Akt phosphorylation at Ser 473 in wild type FVB, K5-UCP3, K5-Akt, and bitransgenic K5-UCP3/K5-Akt epidermal lysates, 4 hours following topical treatment with 2.5 µg TPA or Acetone (vehicle control). Immunoblotting for β-Actin was used to confirm equal loading. (B) Immunohistochemistry for BrdU labeled cells in wild type FVB/N, K5-UCP3, K5-Akt, and bitransgenic K5-UCP3/K5-Akt epidermis following topical treatment with single (1x) or multiple (4x) treatments with 2.5 µg TPA or Acetone. Scale bars = 50 microns. (C) Quantification of BrdU labeled cells in the basal layer of the interfollicular epidermis (IFE). >100 cells from 5 randomly selected skin sections (total >500 cells) were counted from each of n = 3 mice per genotype in each treatment group. Error bars are means +/- SEM. * indicates significantly different from Acetone control, same genotype (** $p<0.01$, *** $p<0.0001$), † indicates significantly different from wild type FVB/N, same treatment (††† $p<0.0001$).

3.3.5 Overexpression of Akt rescues tumorigenesis

Both K5-Akt and K5-UCP3/K5-Akt mice formed more tumors than wild type mice with a modest latency in papilloma multiplicity observed in bi-transgenic animals compared to K5-Akt mice however both groups formed more tumors more rapidly and abundantly compared with wild type mice (Figure 12A-B). Bi-transgenic mice were not resistant to carcinoma formation, developing more carcinomas more quickly than wild type mice however we did observe a reduction in carcinoma formation compared with K5-Akt mice (Figure 12C-D). Collectively this data suggests that Akt inhibition is a critical component to the cancer resistant phenotype seen in K5-UCP3 mice however bi-transgenic mice are still somewhat protected from tumorigenesis compared with K5-Akt mice suggesting that UCP3 may limit tumor progression even with Akt overexpression. Importantly, in this third tumor study no carcinomas were observed on any K5-UCP3 animals providing very strong evidence that uncoupled respiration is incompatible with carcinogenesis (Figure 12 D).

Through these studies we have demonstrated a novel mechanism by which lipid metabolism in keratinocytes regulates cell proliferation through Akt activation. We have proven this mechanism to be cell autonomous and present in both mouse and human keratinocytes indicating the potential of targeting this pathway in human cancers.

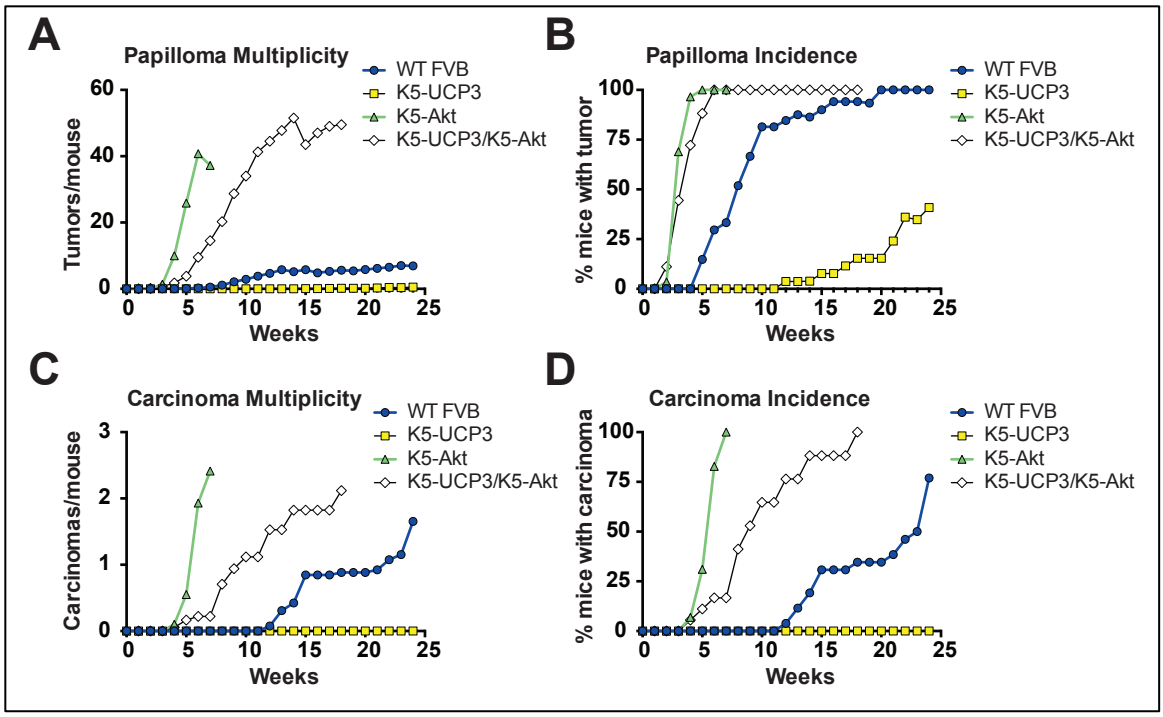

Figure 12. Overexpression of Akt rescues tumorigenesis

(A) Tumor development in wild type FVB, K5-UCP3, K5-Akt, and bitransgenic K5-UCP3/K5-Akt mice indicating total papillomas/mouse, (B) % mice bearing papillomas, (C) total carcinomas/mouse, and (D) % mice bearing carcinomas.

Chapter 4: Final Thoughts

The concepts described within describe two mechanisms that oppose obesity and skin cancer, two of the most common diseases in humans. This data also links many concepts that have been well studied but not well connected by molecular mechanisms. Increasing energy expenditure has long been understood to be a mechanism to lower body weight and oppose obesity however the role of epidermis in this regard has not been well studied. The role that endogenous uncoupling protein expression in the physiological regulation of body weight is not completely clear, which makes models like the K5-UCP3 mouse a valuable asset in obesity research. It is important to note, we did observe UCP3 overexpression in other tissues in which keratin 5 is endogenously expressed, such as bladder, lung, forestomach, pancreas and esophagus. Although we chose to focus on epidermis as it relates to control of systemic metabolism, we cannot rule out effects of UCP3 overexpression in oral cavity, esophagus and forestomach specifically due to the exposure to dietary nutrients in contributing to the anti-obesity phenotype of K5-UCP3 mice. We can use the data here to compare the functions of overexpression of UCP3 in epidermis to models where it is overexpressed in skeletal muscle to compare and contrast the roles that these two tissues play in regulating overall body weight. Furthermore, we can compare studies with ectopic expression of UCP1 in adipose tissue and skeletal muscle with the effects of UCP3 overexpression to understand what mechanisms are activated by uncoupling proteins in those tissues and how they may be targeted therapeutically.

Our data here demonstrate that UCP3 overexpression in epidermis increases glycolysis and fatty acid oxidation through upregulation of Glut1 and activation of AMPK. This phenotype is very similar to the effects of overexpression of UCP3 or UPC1 in skeletal muscle which also improve glucose tolerance and oppose obesity[44,47,67,78]. This suggests that both proteins may activate a similar mechanism to increase skeletal muscle energy expenditure. Interestingly, if these studies are compared to ectopic expression of UCP1 in white adipocytes or in liver, a common mechanism activated by uncoupling that can induce effects on whole body metabolism. Specifically, UCP1 overexpression in white fat, muscle or liver leads to reduced body weight after high fat diet, increased overall energy expenditure, reduced plasma insulin and increased glucose tolerance. These phenotypes are similar to what is known about the role of AMPK activation in these tissue and the differences in phenotypes between the three models are similar to the effects of tissue specific AMPK activation[8].

The general function of active AMPK is to increase nutrient uptake and energy production and to inhibit processes that consume large amounts of ATP[79]. One example of how this occurs is through inhibition of acetyl CoA carboxylase (ACC) which converts cytoplasmic acetyl CoA to malonyl CoA in one of the first steps of *de novo* lipid synthesis[80,81]. ACC inhibition also serves a function in increasing fatty acid oxidation since its product, malonyl CoA, acts as an endogenous inhibitor of carnitine palmitoyl transferase 1 (CPT1) in the carnitine shuttle for fatty acid oxidation[69]. Fatty acids are imported into mitochondria using the carnitine shuttle and are oxidized in the matrix through β-oxidation enzymes, and normal physiological increases in cytoplasmic malonyl

CoA inhibit CPT1 from importing newly synthesized lipids into mitochondria for oxidation during activation of *de novo* lipid synthesis. Thus, AMPK inhibition of ACC represents a major regulatory point in cellular lipid metabolism and phosphorylation states of both proteins can be used as an indicator for evaluating lipid synthesis and oxidation. The effects of AMPK activation and ACC inhibition by UCP3 overexpression in epidermis have similar effects on systemic metabolism with skin–specific *Scd1* knockout mice. This suggests that inhibition of lipid synthesis in epidermis through Scd1 knockout, AMPK activation or ACC inhibition may be sufficient to influence whole body metabolism.

AMPK activation also promotes increased glucose uptake and glycolysis which is a quick and relatively effective mechanism to restore cellular ATP levels and energy homeostasis. AMPK activation promotes translocation of GLUT proteins to the plasma membrane to increase glucose uptake and phosphorylates glycolytic enzymes to facilitate effective ATP synthesis from glycolysis. Contraction in skeletal muscle leads to AMPK activation both *in vivo* and *ex vivo* and multiple studies have demonstrated that this leads to increased GLUT4 translocation to the plasma membrane and increased glucose uptake[82-85]. Furthermore, this mechanism requires the AMPK upstream kinase, LKB1 since glucose uptake is abolished when LKB1 is ablated specifically in skeletal muscle[86]. Interestingly, it has been suggested that long-chain fatty acid esters might inhibit AMPK activation suggesting a feed back mechanism to limit AMPK activation when fatty acids are increased[87]. Thus AMPK activation is likely integral to the metabolic profile induced

by UCP3 overexpression in epidermis and more needs to be investigated about epidermal AMPK activation as a potential target for treating obesity.

The second mechanism discussed herein demonstrates novel metabolic regulation of Akt and keratinocyte proliferation. With UCP3 overexpression, increased lipid oxidation leads to phospholipid breakdown, reduced membrane recruitment, and reduced activation of Akt. Keratinocytes will degrade phospholipids when grown in the absence of glucose which suggests that this mechanism may be specific to epidermis since other tissues may increase fatty acid uptake under energy limiting conditions[88]. We investigated whether high fat diet might rescue UCP3-induced Akt inhibition however transgenic mice fed a high fat diet maintained Akt inhibition in epidermis (data not shown). This suggests that inhibition of lipid synthesis or depletion of specific lipid species may be critical to recapitulating this mechanism to inhibit cancer growth.

Many studies have demonstrated the presence of lipid rafts in cellular membranes that are critical for activation of signaling cascades that initiate with extracellular ligand binding transmembrane receptors like EGFR. Specifically, Akt has been shown to co-localize with detergent-resistant lipid rafts in keratinocyte membranes[89] and two separate studies have indicated Akt is more effectively activated when located in lipid-raft regions[90,91]. Disruption of membrane fluidity with cholesterol depleting agents results in rapid inactivation of Akt providing additional evidence that membrane composition requirements are essential for maximal Akt activation[89]. These studies provide a framework for further investigation into how UCP3 overexpression inhibits Akt activation through increasing lipid oxidation in epidermis. A deeper understanding of the

specific lipid oxidative pathways that degrade phospholipids in K5-UCP3 epidermis would provide an informed context for developing therapeutics to target this mechanism in skin cancers

Chapter 5: Materials and Methods

Reagents.

Glucose (50% dextrose/water) and insulin (Humulin R) were purchased from Animal Health International (Greeley, CO). 12-O-tetradecanoylphorbol-13-acetate (TPA) and okadaic acid (OA) were purchased from LC Laboratories (Woburn, MA). Etomoxir ethyl ester (Eto) was purchased from US Biological (Salem, MA). Acetone, 7,12-dimethylbenz[a]anthracene (DMBA), and all other reagents (unless otherwise noted) were purchased from Sigma (St. Louis, MO)

.

Animals.

K5-UCP3 (FVB/N) mice were generated as previously described [25] using a bovine keratin 5 promoter and murine UCP3 construct and maintained as hemizygous breeder colonies with FVB/N mice purchased from Jackson Laboratories (Bar Harbor, ME). All experiments were performed in male littermates at either 6-9 weeks old or 15-18 weeks old (diet studies) housed under a 12-hour light-dark cycle with ad libitum access to food and water; in accordance with the guidelines defined by the Association for Assessment and Accreditation of Laboratory Animal Care (AAALAC) with approval from the Institutional Animal Research Committees at The University of Texas at Austin and UT-MD Anderson Science Park Research Division. Unless otherwise specified, mice were weaned at 3 weeks old onto Prolab RMH 1800 chow diet from LabDiet (St. Louis, MO).

All metabolic measurements, unless other specified were performed under ad lib feeding with consideration for diurnal metabolic effects.

Caloric intake and body composition analysis.

Body weight measurements were performed upon weaning and mice were weighed once per week. Caloric intake in mice on chow diet (Figure 2B) was measured by weighing food once per day for a period of 3 days (N=10 per genotype). Body composition in mice on chow diet (Figure 2C) was performed using dual-energy X-ray absorptiometry (DEXA) using a Piximus II (GE Healthcare Lunar) (numbers of mice used: FVB/N N=4, K5-UCP3 N=5).

High fat diet studies.

Mice used for diet studies were littermates weaned onto either control diet (D12450) or 60% kcal high fat diet (D12492) both from Research Diets (New Brunswick, NJ). Body weight and caloric intake were measured once per week. (numbers of mice used: FVB/N CD N=21, FVB/N HF N=19, K5-UCP3 CD N=20, K5-UCP3 HF N=14). Body composition analysis in mice on control and high fat diet was performed using an EchoMRI 100H (Houston, TX) (numbers of mice used: FVB/N CD N=6, FVB/N HF N=5, K5-UCP3 CD N=6, K5-UCP3 HF N=6)

Glucose and insulin Tolerance Tests.

For glucose and insulin tolerance tests, mice were fasted overnight (14-16 hours) and fasting blood glucose measurements were taken using a TrueTrack® glucometer (Nipro Diagnostics, Fort Lauderdale, FL) via tail tip. Mice were then given an intraperitoneal injection of either 2g/kg glucose or 0.75U/kg insulin and blood glucose levels were monitored via the tail tip over the period of 2-3 hours. Area under the curve measurements were calculated using the trapezoid rule. (numbers of mice used: GTT, FVB/N N=20, K5-UCP3 N=14, ITT, FVB/N N=5, K5-UCP3 N=5).

Serum Insulin and NEFA levels.

Fasting insulin and NEFA levels were measured in serum from overnight fasted (14-16 hours) mice (N=5). Mice were sacrificed by isoflurane exposure followed by cardiac puncture for blood collection. Blood was allowed to coagulate at 4°C for 1-2 hours followed by centrifugation at 3000 x g for 15 minutes and serum was removed and flash frozen in liquid nitrogen and stored at -80°C until further analysis. Fasting insulin levels were detected using an Insulin ELISA (EMD Millipore, Billerica, MA).

Lactate Dehydrogenase Assay.

Lactate secretion was measured from isolated primary keratinocytes using a lactate colorimetric assay (BioVision, Milpitas, CA). Briefly, primary keratinocytes were isolated as described previously (full protocol in Appendix A) and grown in Eagle's Minimal Essential Medium-2 (Invitrogen, Carlsbad, CA) supplemented with 1% FBS

(0.05mM Ca2+). Lactate levels were measured in the media after 1 hour incubation with primary cells and normalized to total protein.

Gene Expression in Epidermis.

Epidermis was isolated from ad libitum fed mice and mice fasted 14-16 hours (full protocol in Appendix A). Briefly, mice were sacrificed via CO2 exposure followed by cervical dislocation, shaved on the dorsal surface followed by treatment with a depilatory agent. Dorsal skin samples were excised, subcutaneous fat removed and discarded. Epidermal tissue was collected and flash frozen in liquid nitrogen and stored at -80°C until further analysis. Tissue was ground under liquid nitrogen using a mortar and pestle and homogenized in TRI Reagent (Sigma-Aldrich, St. Louis, MO) with a dounce homogenizer. RNA was extracted according to TRI reagent protocol and cDNAs were created using 2µg total RNA per reaction with MMLV-RT (Life Technologies, Grand Island, NY). Real-time PCR was performed using iTaqΠ™ Universal SYBR® Green Supermix in a CFX96 Real-Time PCR Machine (Bio-Rad, Hercules, California). Primer sequences are listed in Appendix B.

Immunoblotting.

Epidermal tissue or whole cell lysates were prepared by lysis in RIPA buffer (50 mM Tris-HCl, 1% NP-40, 0.5% Na Deoxycholate, 0.1% SDS, 150 mM NaCl, 2 mM EDTA) supplemented with protease and phosphatase inhibitor cocktails (Roche, Nutley, NJ). For membrane localization experiment, tissue fractionation was performed using differential

centrifugation and density gradients as described[92]. Protein lysates were separated by SDS-PAGE and transferred to nitrocellulose. Blots were probed with the following primary antibodies: α-phospho Akt S473, α-phospho Akt T308, α-Akt, α-phospho FOXO1 S256, α-phospho FOXO1 S319, α-phospho GSK-3β S9, α-GSK-3β, α-phospho TSC2 S939, α-phospho mTOR S2448, α-phospho mTOR S2481, α-mTOR, α-phospho 4EBP1 T36/47, α-4EBP1, α-phospho rs6 T240/244, α-rS6, α-phospho eIF4G S1108, α-phospho EGFR Y1086, α-EGFR, α-phospho p38 MAPK T180/Y182, α-p38 MAPK, α-PTEN, α-PP2Ac, α-PP2Aa, α-phospho ERK T202/Y204, α-ERK, α-phospho p90 RSK T359/S363, α-p90 RSK, α-β-Actin, (Cell Signaling Technology, Danvers, MA), α-Cyclin D1, α-Cyclin A, α-p21, α-p27, α-α tubulin (Santa Cruz Biotechnology, Dallas, TX), α-α3 Integrin (Chemicon, Billerica, MA), and α-UCP3 (Washington Biotechnology, Simpsonville, MD). Following primary antibody, blots were incubated with α-rabbit-HRP or α-mouse-HRP (GE Healthcare, Piscataway, NJ), and developed using chemiluminescent substrate (Thermo Scientific, Rockford, IL). Results are representative of three separate experiments.

Metabolomic Analysis.

For metabolic profiling, mice (n=6 per genotype) were fasted for 5 hours prior to sample collection to control for metabolic variation due to feeding, then sacrificed via cervical dislocation. Dorsal skin biopsies were taken and epidermal tissue was harvested as

described above. Samples were flash frozen in liquid N2 and stored at -80°C until processed.

Unbiased metabolomic profiling analysis was performed by Metabolon (Durham, NC) as described elsewheret[93]. Briefly, samples were prepared with the automated MicroLab STAR system from Hamilton Company using an aqueous methanol extraction process to remove proteins while allowing maximum recovery of small molecules. Aliquots of the resulting extract were analyzed by ultrahigh performance liquid chromatography/mass spectrometry (UPLC/MS/MS; positive mode), UPLC/MS/MS (negative mode), or GC/MS. Raw data were extracted, peak identified, processed against quality control standards, and normalized to total protein content by Metabolon. Compounds were identified by comparison with a library of >2,400 purified standards' analytical characteristics on Metabolon's LC and GC platforms. Compounds with a p-value <0.05 in a Welch's two-sample t-test were considered to be significantly different between genotypes.

Tumor experiments.

For Tg.AC tumor experiment, 16 week-old mice (Tg.AC n=20, K5-UCP3/Tg.AC n=20) were shaved dorsally and treated with biweekly applications of TPA (2.5 μg) for two weeks for a total of 4 treatments, as described elsewhere[75]. For K5-UCP3/K5-Akt rescue experiment, adult (6-8-week) WT FVB/N (n=28) and hemizygous K5-UCP3 (n=27), K5-Akt (n=29), and K5-UCP3/K5-Akt (n=18) littermates were initiated topically on shaved

dorsal skin with a single application of DMBA (100 μg) followed two weeks later with biweekly applications of TPA (2.5 μg) for 26 weeks, as previously described[94]. In both experiments, mice were scored weekly for tumor incidence (percentage of mice with skin tumors) and tumor multiplicity (number of skin tumors per mouse). Mice were sacrificed if moribund, if any individual tumor reached a diameter of >1 cm, or at the termination of the experiment.

Topical treatments

For all experiments involving topical application of chemicals, mice were shaved on dorsal skin 48 hours prior to treatment. Two to four animals per group were used for each experiment. Mice were treated topically with 200μL acetone (vehicle control), 12.5 μg/mL TPA (2.5 μg dose), 25 mM OA (5 nmol dose), or 5 mg/mL Eto (1 mg dose) and sacrificed at the indicated time points.

5-bromo-2-deoxyuridine (BrdU) labeling & histology

24 hours after acetone or single TPA treatment, mice were injected i.p. with 10 mg/kg BrdU in sterile saline, then sacrificed 30 minutes after injection. For 4x TPA treatment, mice received biweekly treatments for 2 weeks (total of 4 treatments), and were injected with BrdU and sacrificed 48 hours after the final TPA treatment. Dorsal skin biopsies were collected and fixed overnight in 10% neutral buffered formalin, moved to 70% ethanol, and embedded in paraffin. Sections were stained as previously described[95]. Labeling index was calculated as the percentage of basal epidermal cells positive for

BrdU. >100 cells from 5 randomly selected skin sections (total >500 cells) were counted from each of n = 3 mice per genotype in each treatment group.

PP2A activity assay

PP2A was immuno-precipitated using primary α-PP2Ac (Millipore, Billerica, MA), incubated with a target phospho-peptide, and free phosphate release was measured via Malachite Green assay per the manufacturer's instructions (Millipore, Billerica, MA).

Primary cell cultures & signaling experiments

All cell lines were cultured under standard conditions of 5% CO2, 37°C. Primary mouse keratinocytes were harvested from the dorsal skin of adult mice and cultured as previously described[96]. For signaling experiments, cells were grown in EMEM-2 with 1% FBS for 48-72 hours following isolation, then starved overnight (~18 hours) before treatment. Primary neonatal human keratinocytes (NHK) were isolated as previously described[97] and cultured in Keratinocyte Serum Free Media (KSFM, Life Technologies, Grand Island, NY) for no more than 5 passages. Transfections were performed using Lipofectamine 2000 reagent (Life Technologies, Grand Island, NY), and signaling experiments were performed 72 hours after transfection. NHK were moved to KSFM without epidermal growth factor (EGF) and bovine pituitary extract (BPE) supplements 18 hours prior to treatment with 40 ng/mL EGF (Gemini Bioproducts, West Sacramento, CA) or 0.0001% BSA (vehicle control, Fisher Scientific, Pittsburgh, PA), incubated at

37°C, 5% CO2 until the indicated time point, then harvested and used for immunoblotting as described below.

Statistics.

Data are expressed as mean ± SEM. Repeated measures experiments (weights per week, caloric consumption, GTT, and ITT) were analyzed using a two way ANOVA followed by Tukey's post hoc analysis using GraphPad Prism. Gene expression analysis and diet experiments were also analyzed by two way ANOVA followed by Tukey's post hoc while analysis between genotypes was performed using the student's t-test. Statistical significance was determined by a $p < 0.05$.

Appendices

I. Isolation of primary keratinocytes from murine epidermis

Reagents:

Collagen Coating (store at 4°C)

MCDB 151 -100mL: Irvine Sci (Catalog # 9061 or M6645)
Fibronectin-1mg: Sigma (Catalog # F-4759)
PureCol – 1mL: Inamed Biomaterials (Catalog # 5409)
BSA-10mg: Sigma (Catalog # A-3156)
HEPES- 1mL of 2M HEPES: Sigma (Catalog # H-9135)

Trypsin (store at 4°C – invert before use)
Gibco (catlog #15090-046); dilute 1:10 in PBS prior to use.

22.5% Percoll (store at 4°C)
100% Percoll: Pharmacia (Catalog # 17-0891-01, sterile)

For 400mL:
90mL Percoll
10mL 1N NaCl (sterile)
300mL PBS

EMEM base medium (1L)

NaCl – 6.72 g
KCl – 398 mg
D-glucose – 1g
$NaP0_4$ monobasic – 126.5 mg
$MgSO_4$ hexahydrate – 185 mg
Phenol Red – 10 mg
$NaHCO_3$ – 2.25 g
L-Glutamine (200mM) – 10mL
MEM non-essential amino acids (100x Sigma) – 10mL
MEM amino acids (50x Sigma) – 20mL
MEM vitamins (100x Sigma) – 10mL
ddH_20 – 950mL

EMEM #2 Supplements

Calcium chloride – 0.05mM final
EGF – 5ng/mL final
Ethanolamine – 10uM final
FBS – 1 % final
L-Glutamine -1mM final (not including what is in the base)
HEPES – 10mM final
Insulin – 5µg/mL
Penicillin/Streptomycin – 100U/mL
O-Phosphoethanolamine - 10µM
Transferrin - 10µg/mL

Procedure:

1. Prepare sterile materials in the biosafety cabinet:

a. Sterile forceps (2), scissors, #22/23 scalpel, polypropylene monofilament mesh (Small Parts Inc. catalog # CMP149-C) – 1 per genotype, small stir bars – 1 per genotype.
b. 50mL beaker containing 30mL PBS + 1mL Pen/Strep – one per genotype
c. plastic petri dishes (100mm) – one per mouse
d. glass petri dishes (100mM) - one per 3 mice
e. 1X trypsin (diluted PBS) – 15mL per glass dish

2. Prepare materials outside of biosafety cabinet:

a. Large beaker with betadine (~100mL)
b. 70% ethanol – (~300mL for washing)
c. Clippers and Nair for hair removal

3. Sacrifice mice and use clippers to remove dorsal hair then apply Nair for about 1 min.

4. Wash the mouse with tap water to remove Nair and hair then place whole mouse in beaker with betadine. Rinse mice with betadine and then with tap water until water is clear.

5. Rinse mice twice with 70% ethanol (do not rinse with water after this). Dry animals with absorbent pad and transfer to the biosafety cabinet.
6. Using sterile scissors and forceps remove dorsal skin from each mouse and place in beaker with PBS and Pen/Strep. Keep genotypes in separate beakers.

7. One skin at a time, remove from PBS/Pen/Strep and place skin hair side down in a plastic petri dish. Use scalpel to remove subcutaneous fat. Make long consistent strokes

and scrape at a consistent depth across each piece of skin. (It is important to remove all fat for subsequent steps)

8. Transfer skin to a clean petri dish and place hair side up (flip the skin over). Spread the skin out and allow to dry for 3-5 min.

9. Transfer skin (still hair side up) to a glass petri dish containing 15mL 1X trypsin. Skin should float on top of liquid. Avoid air bubbles between skin and trypsin and avoid trypsin on top of the skin samples. Up to 3 skins can fit in one petri dish, keep genotypes separate.

10. Place skins in incubator – time and temperature varies based on procedure:

> a. Oximetry in whole epidermis: 30°C for 1 hour and 30-45 minutes. Shorter times make collecting whole sheets of epidermis difficult, longer times reduce epidermal respiration and increase cell dissociation from epidermal sheet.
>
> b. Isolation of primary keratinocytes: 30°C for 2 hours or 1 hour at 37°C and one hour at room temperature. Not much differs between theses methods in terms of efficiency. 2 hours at 37°C can decrease final cell yield.

11. Remove skins from incubator and place in biosafety cabinet. Prop one edge of a petri dish up and add 4mL EMEM #2 (10% FBS) to the dish. Lightly rinsing the petri dish with the media will allow the skin to slide, making it easier to handle. Spread the skin out flat (hair side up) and use a scalpel to scrape epidermis off in sheets. Collect epidermis in pooled media at the bottom of petri dish. Use the same dish for all skin from each genotype.

12. Carefully transfer epidermis from perti dish into a 50mL beaker and rinse petri dish to collect remaining cells with 7mL EMEM #2 (10% FBS) and collect in beaker.

13. Mince the epidermis with scissors for 5 minutes each. With 30mL EMEM #2 (10% FBS) rinse scissors and collect extra cells in 50mL beaker. Add small stir bar and cover beaker with sterile foil. Place beaker on stir plate and stir gently for 30 min.

14. Filter samples through mesh using a sterile glass funnel into a 50mL conical tube. Spin cells at 250 x g for 10min at 4°C.

15. Remove supernatant and resuspend pellets in 2mL EMEM #2 (10% FBS). This is 2mL/percoll gradient, no more than 6 mice should be used on a single percoll gradient. Resuspend this pellet well as a single cell suspension is best for the percoll gradient.

16. Add 20mL cold 22.5% percoll to a 50mL tube, overlay the cell suspension on the percoll by adding very slowly to the 50mL tube while at a 45 degree angle.

17. Spin percoll gradient at 250 x g with slow acceleration and no break for 15 minutes at 4°C. Remove supernatant and take care not to disrupt the loose pellet.

18. Resuspend pellet in 10mL EMEM #2 (1% FBS) and then spin at 250 x g at 4°C and remove supernatant. This step removes excess percoll. Resuspend final pellet in EMEM #2 (1% FBS). Resuspension volume can be anything less than 10mL.

19. Count cells and plate on collagen coated plates. Wash cells with PBS and change media the next day to remove dead cells. 2-3 million cells per 6-well plate will be confluent within 48-72 hours after initial plating.

I. ISOLATION OF PRIMARY KERATINOCYTES FROM HUMAN FORESKIN SAMPLES

Reagents:

Keratinocyte Serum Free Media (Gibco) - supplemented with bovine pituitary extract and EGF. Store at 4°C.

HBSS Solution – sterile

50mL HBSS (10x w/o Bicarb, Gibco #14060-057)
5mL 7% Sodium Bicarbonate (tissue culture grade)
5mL of 1M HEPES
440mL ddH_2O

Dispase Solution – filter sterilize and store at 4°C.

50mL HBSS Solution
5µl Gentamicin (50mg/mL stock - 5 µg/mL final)
2µ Fungizone (250µg/mL)
500mg Dispase (Final 10mg/mL)

Stop Media – sterile, store at 4°C

DMEM culture media
10% FBS
1% Pen/Strep
0.1% Gentamicin

Preparation for sample collection:

Place 5mL EMEM #2 media + 1:10,000 dilution of Gentamicin (50mg/mL)
Deliver tubes to charge nurse, pick up new samples.

Procedure:

1. Use sterile scissors and forceps in a biosafety cabinet.

2. Place 2-3mL Dispase Solution in 6-well plates.

3. Place sample in petri dish and flatten out foreskin by trimming subcutaneous fat. If necessary, cut sample into pieces 1-2 cm pieces.

4. Float flattened skin on dispase solution. Sample may curl under which is okay.

5. Cover and place plates at 4°C overnight (16-18 hours), longer will decrease viability.

6. Use sterile forceps in a biosafety cabinet. Transfer skin to a petri dish and use forceps to peel epidermis from the dermis. Place epidermis in a 50mL tube containing 2-3mL trypsin-EDTA (0.25% Trypsin, 1mM EDTA). Swirl to immerse tissue and place at 37°C for 5-7 minutes. Gently swirl half way through incubation.

7. Add 25-30mL Stop media, swirl to mix. Centrifuge at 3000 x g for 10 minutes at 4°C.

8. Remove supernatant along with any floating tissue. Resuspend cells in 10mL KSFM. Resuspend very well as cell viability is increased when cells are plated in a single cell suspension.

9. Plate cells in 10 cm dishes. One sample plated in a single 10 cm dish will usually be confluent in 1-2 days, samples can be spread between several 10 cm plates however lower levels of confluence will reduce the rate of proliferation of cells.

Transfection of NHK cells:

Cells are transfected in suspension so set up DNA complexes first and then split cells. Complexes will be ready by the time the cells are ready to plate. Transfections are described for 10cM plates transfected with 5-10µg DNA total and a lipofectamine:DNA ratio of 3:1.

1. Pre-warm KSFM (no supplements) and bring all other reagents to room temperature.

2. Prepare DNA stocks to 1 or 2µg/µl.

3. Dilute DNA in 500µl KSFM (no supplements), add lipofectamine 3000 and p3000 reagent according to manufacturers recommendations. Allow DNA to complex at room temperature for 15-30 minutes.

4. Plate cells 1.2-1.5 million cells per 10cm dish. Add complexed DNA dropwise and swirl plate to mix. Place plates in 37°C incubator. Remove media and wash cells with PBS 6 hours after transfection and replace with fresh KSFM media.

References

1. Bray, G. A. & Tartaglia, L. A. Medicinal strategies in the treatment of obesity. *Nature* **404,** 672–677 (2000).
2. Kozak, L. P., Koza, R. A. & Anunciado-Koza, R. Brown fat thermogenesis and body weight regulation in mice: relevance to humans. *Int J Obes (Lond)* **34,** S23–S27 (2010).
3. Goldgof, M. *et al*. The chemical uncoupler 2,4-dinitrophenol (DNP) protects against diet-induced obesity and improves energy homeostasis in mice at thermoneutrality. *J. Biol. Chem.* **289,** 19341–19350 (2014).
4. Rai, M. & Demontis, F. Systemic Nutrient and Stress Signaling via Myokines and Myometabolites. *Annu. Rev. Physiol.* **78,** 85–107 (2016).
5. Cao, H. *et al*. Identification of a Lipokine, a Lipid Hormone Linking Adipose Tissue to Systemic Metabolism. *Cell* **134,** 933–944 (2008).
6. Hue, L. & Taegtmeyer, H. The Randle cycle revisited: a new head for an old hat. *AJP: Endocrinology and Metabolism* **297,** E578–E591 (2009).
7. Saltiel, A. R. & Kahn, C. R. Insulin signalling and the regulation of glucose and lipid metabolism. *Nature* **414,** 799–806 (2001).
8. Klaus, S., Keipert, S., Rossmeisl, M. & Kopecky, J. Augmenting energy expenditure by mitochondrial uncoupling: a role of AMP-activated protein kinase. *Genes Nutr* **7,** 369–386 (2012).
9. Mueckler, M. Facilitative glucose transporters. *Eur. J. Biochem.* **219,** 713–725 (1994).
10. Herzig, S. *et al*. Identification and Functional Expression of the Mitochondrial Pyruvate Carrier. *Science* **337,** 93–96 (2012).
11. McGarry, J. D. & Brown, N. F. The Mitochondrial Carnitine Palmitoyltransferase System — From Concept to Molecular Analysis. *European Journal of Biochemistry* **244,** 1–14 (1997).
12. Lodish, H. *et al*. Electron Transport and Oxidative Phosphorylation. (2000).
13. Cannon, B. Brown Adipose Tissue: Function and Physiological Significance. *Physiological Reviews* **84,** 277–359 (2004).
14. Hopfer, U. & Lehninger, A. L. Protonic conductance across phospholipid bilayer membranes induced by uncoupling agents for oxidative phosphorylation. in (1968).
15. Palmieri, F. The mitochondrial transporter family (SLC25): physiological and pathological implications. *Pflugers Arch - Eur J Physiol* **447,** 689–709 (2004).
16. Spiegelman, J. W. P. B. L. S. L. Y. J. C. A.-H. G. M. K. K. V. P. N. G. S. K. H. H. T. W. V. J. H. S. E. P. S. B. *et al*. Beige Adipocytes Are a Distinct Type of Thermogenic Fat Cell in Mouse and Human. *Cell* **150,** 366–376 (2012).
17. Bartesaghi, S. *et al*. Thermogenic Activity of UCP1 in Human White Fat-Derived Beige Adipocytes. *Mol. Endocrinol.* **29,** 130–139 (2015).

18. Feldmann, H. M., Golozoubova, V., Cannon, B. & Nedergaard, J. UCP1 Ablation Induces Obesity and Abolishes Diet-Induced Thermogenesis in Mice Exempt from Thermal Stress by Living at Thermoneutrality. *Cell Metabolism* **9,** 203–209 (2009).
19. Wang, Q. *et al*. Brown Adipose Tissue Activation Is Inversely Related to Central Obesity and Metabolic Parameters in Adult Human. *PLOS ONE* **10,** e0123795–13 (2015).
20. Schrauwen, P. & Hesselink, M. UCP2 and UCP3 in muscle controlling body metabolism. *J. Exp. Biol.* **205,** 2275–2285 (2002).
21. Vidal-Puig, A. *et al*. Effects of obesity and stable weight reduction on UCP2 and UCP3 gene expression in humans. *Obes. Res.* **7,** 133–140 (1999).
22. Fleury, C. *et al*. Uncoupling protein-2: a novel gene linked to obesity and hyperinsulinemia. *Nat. Genet.* **15,** 269–272 (1997).
23. Boss, O. *et al*. Uncoupling protein-3: a new member of the mitochondrial carrier family with tissue-specific expression. *FEBS Letters* **408,** 39–42 (1997).
24. Vidal-Puig, A., Solanes, G., Grujic, D., Flier, J. S. & Lowell, B. B. UCP3: an uncoupling protein homologue expressed preferentially and abundantly in skeletal muscle and brown adipose tissue. *Biochem. Biophys. Res. Commun.* **235,** 79–82 (1997).
25. Lago, C. U. *et al*. Mitochondrial respiratory uncoupling promotes keratinocyte differentiation and blocks skin carcinogenesis. *Oncogene* **31,** 4725–4731 (2012).
26. Vozza, A. *et al*. UCP2 transports C4 metabolites out of mitochondria, regulating glucose and glutamine oxidation. *Proc. Natl. Acad. Sci. U.S.A.* **111,** 960–965 (2014).
27. Bouillaud, F., Alves-Guerra, M.-C. & Ricquier, D. UCPs, at the interface between bioenergetics and metabolism. *BBA - Molecular Cell Research* 1–14 (2016). doi:10.1016/j.bbamcr.2016.04.013
28. Qian, L. *et al*. UCP2 -866G/A, Ala55Val and UCP3 -55C/T polymorphisms in association with obesity susceptibility - a meta-analysis study. *PLOS ONE* **8,** e58939 (2013).
29. Salopuro, T. *et al*. Variation in the UCP2 and UCP3 genes associates with abdominal obesity and serum lipids: the Finnish Diabetes Prevention Study. *BMC Med. Genet.* **10,** 94 (2009).
30. Ochoa, M. C. *et al*. Association between obesity and insulin resistance with UCP2-UCP3 gene variants in Spanish children and adolescents. *Mol. Genet. Metab.* **92,** 351–358 (2007).
31. Walder, K. *et al*. Association between uncoupling protein polymorphisms (UCP2-UCP3) and energy metabolism/obesity in Pima indians. *Hum. Mol. Genet.* **7,** 1431–1435 (1998).
32. Alonso, A. *et al*. Association of UCP3 gene -55C>T polymorphism and obesity in a Spanish population. *Ann. Nutr. Metab.* **49,** 183–188 (2005).
33. de Luis, D. A. *et al*. [Relation of -55CT polymorphism of UCP3 gene with weight loss and metabolic changes after a high polyunsaturated fat diet in obese

patients]. *Nutr Hosp* **27,** 1190–1195 (2012).
34. Oliveira, B. A. P. *et al*. UCP1 and UCP3 Expression Is Associated with Lipid and Carbohydrate Oxidation and Body Composition. *PLOS ONE* **11,** e0150811–11 (2016).
35. Kaisaki, P. J., Woon, P. Y., Wallis, R. H. & Monaco, A. P. Localization of tub and uncoupling proteins (Ucp) 2 and 3 to a region of rat Chromosome 1 linked to glucose intolerance and adiposity in the Goto-Kakizaki (GK) Type …. *Mammalian …* (1998).
36. Fleury, C., Neverova, M., Collins, S. & Raimbault, S. Uncoupling protein-2: a novel gene linked to obesity and hyperinsulinemia. *Nature* (1997).
37. Gong, D. W. Lack of Obesity and Normal Response to Fasting and Thyroid Hormone in Mice Lacking Uncoupling Protein-3. *Journal of Biological Chemistry* **275,** 16251–16257 (2000).
38. Vidal-Puig, A. J. *et al*. Energy metabolism in uncoupling protein 3 gene knockout mice. *J. Biol. Chem.* **275,** 16258–16266 (2000).
39. Senese, R. *et al*. Uncoupling protein 3 expression levels influence insulin sensitivity, fatty acid oxidation, and related signaling pathways. *Pflugers Arch - Eur J Physiol* **461,** 153–164 (2010).
40. Costford, S. R., Chaudhry, S. N., Crawford, S. A., Salkhordeh, M. & Harper, M. E. Long-term high-fat feeding induces greater fat storage in mice lacking UCP3. *AJP: Endocrinology and Metabolism* **295,** E1018–E1024 (2008).
41. Clapham, J. C. *et al*. Mice overexpressing human uncoupling protein-3 in skeletal muscle are hyperphagic and lean. *Nature* **406,** 415–418 (2000).
42. Gong, D. W., He, Y., Karas, M. & Reitman, M. Uncoupling protein-3 is a mediator of thermogenesis regulated by thyroid hormone, beta3-adrenergic agonists, and leptin. *J. Biol. Chem.* **272,** 24129–24132 (1997).
43. Barbe, P. *et al*. Triiodothyronine-mediated up-regulation of UCP2 and UCP3 mRNA expression in human skeletal muscle without coordinated induction of mitochondrial respiratory chain genes. *The FASEB Journal* **15,** 13–15 (2001).
44. Bezaire, V. *et al*. Constitutive UCP3 overexpression at physiological levels increases mouse skeletal muscle capacity for fatty acid transport and oxidation. *FASEB J.* **19,** 977–979 (2005).
45. MacLellan, J. D. *et al*. Physiological increases in uncoupling protein 3 augment fatty acid oxidation and decrease reactive oxygen species production without uncoupling respiration in muscle cells. *Diabetes* **54,** 2343–2350 (2005).
46. Wang, S., Subramaniam, A., Cawthorne, M. A. & Clapham, J. C. Increased fatty acid oxidation in transgenic mice overexpressing UCP3 in skeletal muscle. *Diabetes Obes Metab* **5,** 295–301 (2003).
47. Neschen, S. *et al*. Uncoupling protein 1 expression in murine skeletal muscle increases AMPK activation, glucose turnover, and insulin sensitivity in vivo. *Physiological Genomics* **33,** 333–340 (2008).
48. Kopecky, J., Hodny, Z. & Rossmeisl, M. Reduction of dietary obesity in aP2-Ucp transgenic mice: physiology and adipose tissue distribution. *American*

Journal of … (1996).
49. Feingold, K. R. Thematic review series: skin lipids. The role of epidermal lipids in cutaneous permeability barrier homeostasis. *J. Lipid Res*. (2007).
50. Chuong, C. M., Nickoloff, B. J. & Elias, P. M. What is the'true'function of skin? *Experimental …* (2002). doi:10.1034/j.1600-0625.2002.00112.x
51. ANASTASIA, J. V. & CONLEY, J. P. The role of fatty acid oxidation in the epidermis. *Journal of Investigative Dermatology* (1977). doi:10.1111/1523-1747.ep12510725
52. Wheatley, V. R., Hodgins, L. T. & Coon, W. M. Cutaneous Lipogenesis I. Evaluation Of Model Systems and the Utilization of Acetate, Citrate and Glucose as Compared with other Tissues. *Journal of Investigative Dermatology* **54,** 288–297 (1970).
53. Grubauer, G., Feingold, K. R. & Elias, P. M. *Relationship of epidermal lipogenesis to cutaneous barrier function; 1987. J Lipid Res*
54. Feingold, K. R. The outer frontier: the importance of lipid metabolism in the skin. *J. Lipid Res*. (2009).
55. Hsia, S. L., Dreize, M. A. & Marquez, M. C. Lipid Metabolism in Human Skin. *Journal of Investigative Dermatology* **47,** 443–448 (1966).
56. Wheatley, V. R. Cutaneous Lipogenesis. Major Pathways of Carbon Flow and Possible Interrelationships Between the Epidermis and Sebaceous Glands. *Journal of Investigative Dermatology* **62,** 245–256 (1974).
57. Sampath, H. *et al*. Skin-specific deletion of stearoyl-CoA desaturase-1 alters skin lipid composition and protects mice from high fat diet-induced obesity. *Journal of Biological Chemistry* **284,** 19961–19973 (2009).
58. Flowers, M. T. & Ntambi, J. M. Role of stearoyl-coenzyme A desaturase in regulating lipid metabolism. *Curr. Opin. Lipidol*. **19,** 248–256 (2008).
59. Zheng, Y. *et al*. Scd1 is expressed in sebaceous glands and is disrupted in the asebia mouse. *Nat. Genet*. **23,** 268–270 (1999).
60. Casatorres, J., Navarro, J. M., Blessing, M. & Jorcano, J. L. Analysis of the control of expression and tissue specificity of the keratin 5 gene, characteristic of basal keratinocytes. Fundamental role of an AP-1 element. *Journal of Biological Chemistry* **269,** 20489–20496 (1994).
61. Liang, C.-C., You, L.-R., Chang, J.-L., Tsai, T.-F. & Chen, C.-M. Transgenic mice exhibiting inducible and spontaneous Cre activities driven by a bovine keratin 5 promoter that can be used for the conditional analysis of basal epithelial cells in multiple organs. *J Biomed Sci* **16,** 2–8 (2009).
62. Yamamoto, M., Nakata, H., Kumchantuek, T., Sakulsak, N. & Iseki, S. Immunohistochemical localization of keratin 5 in the submandibular gland in adult and postnatal developing mice. *Histochem. Cell Biol*. **145,** 327–339 (2016).
63. Broede, A. *et al*. Differential diagnosis of bladder versus colorectal adenocarcinoma: keratin 7 and GATA3 positivity in nuclear ß-catenin-negative glandular tumours defines adenocarcinoma of the bladder. *J. Clin. Pathol*. **69,**

307–312 (2016).
64. Wang, X. *et al*. Overexpression of cyclooxygenase-2 (COX-2) in the mouse urinary bladder induces the expression of immune- and cell proliferation-related genes. *Mol. Carcinog*. **48,** 1–13 (2009).
65. Kiguchi, K. *et al*. Constitutive Expression of ErbB-2 in Gallbladder Epithelium Results in Development of Adenocarcinoma. *Cancer Res*. **61,** 6971–6976 (2001).
66. Nowinski, S. M. *et al*. Mitochondrial uncoupling links lipid catabolism to Akt inhibition and resistance to tumorigenesis. *Nat Commun* **6,** 8137 (2015).
67. Costford, S. R. Effects of the presence, absence, and overexpression of uncoupling protein-3 on adiposity and fuel metabolism in congenic mice. *AJP: Endocrinology and Metabolism* **290,** E1304–E1312 (2006).
68. Shen, S., Sampson, S. R., Tennenbaum, T. & Wertheimer, E. Characterization of Glucose Transport System in Keratinocytes: Insulin and IGF-1 Differentially Affect Specific Transporters. *Journal of Investigative Dermatology* **115,** 949–954 (2000).
69. McGarry, J. D., Mannaerts, G. P. & Foster, D. W. A possible role for malonyl-CoA in the regulation of hepatic fatty acid oxidation and ketogenesis. *J. Clin. Invest*. **60,** 265–270 (1977).
70. Hu, C. C., Qing, K. & Chen, Y. Diet-Induced Changes in Stearoyl-CoA Desaturase 1 Expression in Obesity-Prone and -Resistant Mice. *Obes. Res*. **12,** 1264–1270 (2004).
71. Pavlova, N. N. & Thompson, C. B. The Emerging Hallmarks of Cancer Metabolism. *Cell Metabolism* (2016).
72. Bauer, D. E., Hatzivassiliou, G., Zhao, F., Andreadis, C. & Thompson, C. B. ATP citrate lyase is an important component of cell growth and transformation. *Oncogene* **24,** 6314–6322 (2005).
73. Hatzivassiliou, G., Zhao, F., Bauer, D. E. & Andreadis, C. ATP citrate lyase inhibition can suppress tumor cell growth. *Cancer cell* (2005).
74. Digiovanni, J. Multistage carcinogenesis in mouse skin. *Pharmacology & therapeutics* (1992).
75. Battalora, M. S. *et al*. Age-dependent skin tumorigenesis and transgene expression in the Tg.AC (v-Ha-ras) transgenic mouse. *Carcinogenesis* **22,** 651–659 (2001).
76. Manning, B. D. & Cantley, L. C. AKT/PKB signaling: navigating downstream. *Cell* **129,** 1261–1274 (2007).
77. Segrelles, C. *et al*. Deregulated activity of Akt in epithelial basal cells induces spontaneous tumors and heightened sensitivity to skin carcinogenesis. *Cancer Res*. **67,** 10879–10888 (2007).
78. Katterle, Y., Keipert, S., Hof, J. & Klaus, S. Dissociation of obesity and insulin resistance in transgenic mice with skeletal muscle expression of uncoupling protein 1. *Physiological Genomics* **32,** 352–359 (2007).
79. Hardie, D. G., Ross, F. A. & Hawley, S. A. AMPK: a nutrient and energy sensor that maintains energy homeostasis. *Nature Publishing Group* **13,** 251–262

(2012).
80. Winder, W. W. & Hardie, D. G. Inactivation of acetyl-CoA carboxylase and activation of AMP-activated protein kinase in muscle during exercise. *American Journal of Physiology- …* (1996).
81. Witters, L. A. & Kemp, B. E. Insulin activation of acetyl-CoA carboxylase accompanied by inhibition of the 5'-AMP-activated protein kinase. *Journal of Biological Chemistry* (1992).
82. Merrill, G. F., Kurth, E. J., Hardie, D. G. & Winder, W. W. AICA riboside increases AMP-activated protein kinase, fatty acid oxidation, and glucose uptake in rat muscle. *AJP: Endocrinology and Metabolism* **273,** E1107–E1112 (1997).
83. Kurth-Kraczek, E. J., Hirshman, M. F., Goodyear, L. J. & Winder, W. W. 5' AMP-activated protein kinase activation causes GLUT4 translocation in skeletal muscle. *Diabetes* **48,** 1667–1671 (1999).
84. Mu, J., Brozinick, J. T., Valladares, O. & Bucan, M. A role for AMP-activated protein kinase in contraction-and hypoxia-regulated glucose transport in skeletal muscle. *Molecular Cell* (2001).
85. Koistinen, H. A. *et al*. 5-amino-imidazole carboxamide riboside increases glucose transport and cell-surface GLUT4 content in skeletal muscle from subjects with type 2 diabetes. *Diabetes* **52,** 1066–1072 (2003).
86. Sakamoto, K., McCarthy, A. & Smith, D. Deficiency of LKB1 in skeletal muscle prevents AMPK activation and glucose uptake during contraction | The EMBO Journal. *The EMBO …* (2005).
87. Taylor, E. B., Ellingson, W. J., Lamb, J. D., Chesser, D. G. & Winder, W. W. Long-chain acyl-CoA esters inhibit phosphorylation of AMP-activated protein kinase at threonine-172 by LKB1/STRAD/MO25. *AJP: Endocrinology and Metabolism* **288,** E1055–E1061 (2005).
88. Long, V. J. & Yardley, H. J. Phospholipids in cultured guinea pig skin. *Journal of Investigative Dermatology* **54,** 174–177 (1970).
89. Calay, D. *et al*. Inhibition of Akt Signaling by Exclusion from Lipid Rafts in Normal and Transformed Epidermal Keratinocytes. *Journal of Investigative Dermatology* **130,** 1136–1145 (2010).
90. Gao, X. & Zhang, J. Spatiotemporal analysis of differential Akt regulation in plasma membrane microdomains. *Mol. Biol. Cell* **19,** 4366–4373 (2008).
91. Lasserre, R. *et al*. Raft nanodomains contribute to Akt/PKB plasma membrane recruitment and activation. *Nature Chemical Biology* **4,** 538–547 (2008).
92. Cox, B. & Emili, A. Tissue subcellular fractionation and protein extraction for use in mass-spectrometry-based proteomics. *Nat Protoc* **1,** 1872–1878 (2006).
93. Theriot, C. M. *et al*. Antibiotic-induced shifts in the mouse gut microbiome and metabolome increase susceptibility to Clostridium difficile infection. *Nat Commun* **5,** 3114 (2014).
94. Rundhaug, J. E. *et al*. Changes in protein expression during multistage mouse skin carcinogenesis. *Mol. Carcinog.* **20,** 125–136 (1997).
95. Naito, M., Naito, Y. & Digiovanni, J. Comparison of the histological changes in

the skin of DBA/2 and C57BL/6 mice following exposure to various promoting agents. *Carcinogenesis* **8,** 1807–1815 (1987).

96. Morris, R. J., Fischer, S. M., Klein-Szanto, A. J. & Slaga, T. J. Subpopulations of primary adult murine epidermal basal cells sedimented on density gradients. *Cell Tissue Kinet* **23,** 587–602 (1990).

97. Welter, J. F., Crish, J. F., Agarwal, C. & Eckert, R. L. Fos-related antigen (Fra-1), junB, and junD activate human involucrin promoter transcription by binding to proximal and distal AP1 sites to mediate phorbol ester effects on promoter activity. *Journal of Biological Chemistry* **270,** 12614–12622 (1995).